A 4.7 Tesla4-Channel Transmit and Receive MRI Quadrature Birdcage Coil Design and Fabrication for Monkey Head imaging

by

Xiaotong Sun

A thesis submitted to the Graduate Faculty of
Auburn University
in partial fulfillment of the requirements for the Degree of
Master of Science

Auburn, Alabama
August 3, 2013

Keywords: MRI, RF Coil, Quadrature, Hybrid, T/R Switch, Low Noise Amplifier

Approved by

Shumin Wang, Chair, Associate Professor of Electrical and Computer Engineering
MichaelE. Baginski, Associate Professor of Electrical and Computer Engineering
Lloyd S. Riggs, Professor of Electrical and Computer Engineering
Thomas S. Denney Jr., Professor of Electrical and Computer Engineering

Abstract

Magnetic Resonance Imaging (MRI) is an image modality used for clinical diagnosis as well as general imaging research. Functional magnetic resonance imaging or functional MRI (fMRI) is an MRI procedure that measures brain activity by detecting associated changes in blood flow. The study described in this thesis is intended for MRI application. In order to acquire high-resolution MRI images, the signal detector, i.e., radio-frequency (RF) coils plays a pivotal role. In this study, we designed and fabricated a 4.7 Tesla high-pass 4-ch transmit and receive birdcage coil for fMRI monkey head imaging. During RF transmission, this birdcage coil generates a high-uniformity volume excitation which is desired by MRI experiments. During reception, the quadrature nature of the RF output enables an improvement of the signal to noise ratio (SNR) by over 40%. The coil was designed by applying numerical simulations at first. The hardware implementation was done by taking care of tuning, matching and mutual decoupling issues. Also, front end circuits including hybrid, T/R switch and pre amplifier are discussed. MRI images of a saline water phantom acquired with the fabricated coil in a 4.7 Tesla MRI scanner demonstrate a high-degree of excitation homogeneity and SNR, which correspond very well to the theory and numerical simulation results.

Acknowledgments

First of all I would like to thank Dr. Wang for giving me the great opportunity to work in the MRI RF lab and for getting me excited about RF coils and also Dr. Denney, Dr. Riggs and Dr. Baginski for their priceless advice on this work. Moreover, I would like to thank my parents for their unconditional love and support. At last, I would like to thank all the members in our group: Hai Lu, Yu Shao, Ziyuan Fu, Shuo Shang, for their assistance on this project and all the people who have helped me no matter in what ways.

Table of Contents

Abstract ii

Acknowledgments iii

List of Tables vi

List of Figures vii

List of Abbreviations x

Chapter 1 MRI Basics 1

1.1 General Introduction to MRI 1

1.2 Atomic Structure 2

1.3 Basic Spin Manipulation 3

1.4 Signal Detection 8

1.5 Summary 14

Chapter 2 Coil Design and Simulation 15

2.1 Introduction 16

2.2 Theory of Birdcage Coils 17

2.3 Simulation 20

Chapter 3 Front end Circuit Design 30

3.1 Hybrid 31

3.2 T/R Switch 39

3.2 Low Noise Amplifier 44

Chapter 4 Coil Fabrication and Results 49

4.1 Fabrication 49

4.2 Tuning, Matching and Decoupling 50

4.3 Results 52

Chapter 5 Discussion and Future work 57

5.1 Fabrication issues 57

5.2 Future work 58

References 60

List of Tables

Table 1 component value of the hybrid used in the simulation and in reality 41

List of Figures

Figure 1.1 Magnetic dipole moment defined as a circular loop current 4

Figure 1.2 Left: Precession around $\overrightarrow{B_0}$. The red torque vector always points tangentially to the circular motion (because it is the cross product of $\overrightarrow{B_0}$ and $\overrightarrow{M} / \gamma$). Right: Precession around $\overrightarrow{B_0}$ and $\overrightarrow{B_1}$ changes the angle of $\overrightarrow{M}$. The precession now occurs around both $\overrightarrow{B_0}$ and $\overrightarrow{B_1}$ 5

Figure 1.3 Dephasing phenomenon looking down onto the transverse plane 7

Figure 1.5 The X, Y and Z gradient axes 9

Figure 1.6 Slice selection 10

Figure 1.7 Frequency shift 11

Figure 1.8 Phase encoding 12

Figure 1.9 The Fast Fourier Transform 13

Figure 2.1 1) Left: A high-pass birdcage coil with a phantom put inside. 2) Right: With a RF shield put outside 18

Figure 2.2 Lumped element equivalent circuit of a high-pass birdcage coil 19

Figure 2.3 Structure of the cylinder goes inside the 4.7T MRI scanner 21

Figure 2.4 A set of monkey head images with different values in z direction 22

Figure 2.5 A comparison of the coil frame and the monkey head in FEKO 23

Figure 2.6 A comparison of the coil frame, the shield and the monkey head in FEKO 23

Figure 2.7 Birdcage Coil modeled in FEKO with RF shield and phantom 24

Figure 2.8 The frequency spectrum of reflection coefficient 25

Figure 2.9 Different cutting planes. 1) Top: transverse plane. 2) Middle: sagittal plane. 3) Bottom: coronal plane 28

Figure 2.10 B1 field distribution. 1) Top: transverse plane. 2) Middle: sagittal plane. 3) Bottom: coronal plane 29

Figure 2.11 Coil frame modeled in FEKO. 1) Top: Coil frame only. 2) Bottom: Coil and shield frame 30

Figure 3.1 Two commonly used symbols for directional couplers, and power flow conventions 33

Figure 3.2 Quadrature hybrid (or branch-line) coupler 35

Figure 3.3 ADS simulation results. (a) S11 parameter of input Port 1. (b) S41 parameter of output Port 4 36

Figure 3.4 ADS simulation results. (a) S21 parameter of input Port 2 and 1. (b) S31 parameter of output Port 3 and 1 37

Figure 3.5 ADS simulation results. (a) Phase of S21 parameter of input Port 2 and 1. (b) Phase of S31 parameter of output Port 3 and 1. 37

Figure3.6 S11 magnitude (log), S21 magnitude (log) and phase 38

Figure3.7 S11 magnitude (log), S31 magnitude (log) and phase 38

Figure3.8 S11 magnitude (log), S41 magnitude (log) and phase 39

Figure 3.9 Circuit schematic of the combination of hybrid and T/R switch 41

Figure 3.10 Port1: Coil; Port2; RX. S11 magnitude (log), S21 magnitude (log) and phase when DC is OFF) 42

Figure 3.11 Port1: Coil; Port2; RX. S11 magnitude (log), S21 magnitude (log) and phase when DC is ON) 42

Figure 3.12 Port1: TX; Port2; RX. S11 magnitude (log), S21 magnitude (log) and phase when DC is OFF) 43

Figure 3.13 Port1: TX; Port2; RX. S11 magnitude (log), S21 magnitude (log) and phase when DC is ON) 43

Figure 3.14 Port1: TX; Port2; 50ohm. S11 magnitude (log), S21 magnitude (log) and phase when DC is ON) 44

Figure 3.15 Configuration of a 2-stage amplifier design 45

Figure 3.16 Simulation results of the 1st stage LNA. 1) Left: Noise figure. 2) Right: Gain..46

Figure 3.17 Simulation results of the 2nd stage LNA. 1) Left: Noise figure. 2) Right: Gain.46

Figure 3.18 Simulation results of the overall 2-stage LNA. 1) Left: Noise figure. 2) Right: Gain 47

Figure 3.19 DC Biasing Circuit 48

Figure 3.20 Bench testing results. Noise figure and Gain of the amplifier..... 49

Figure 4.1 Coil frame printed out by 3d printer 51

Figure 4.2 The end-ring configuration of the birdcage coil with match and tuning capacitors…. 52

Figure 4.3 Benching testing results. (a) S11 of port1 (b) S11 of port2 (c) S21 54

Figure 4.4 The birdcage coil and a water phantom inside the MRI scanner. (a) Front side view (b) back side view 55

Figure 4.5 MRI images. 1) left: transverse plane. 2) middle: coronal plan. 3) right: sagittal plane 57

Figure 4.6 A comparison of the previous simulation results 57

Figure 5.1 An 8-ch transmit and receive phased array coil 60

List of Abbreviations

MRI	Magnetic Resonance Imaging
fMRI	functional Magnetic Resonance Imaging
RF	Radio Frequency
QM	Quantum mechanical
SNR	Signal-to-Noise Ratio
TX	Transmit
RX	Receive
PIN	Positive-Intrinsic-Negative
FDTD	finite-difference-time-domain
DCB	DC Block
RFC	RF Chock
FFT	Fast Fourier Transform
LNA	Low Noise Amplifier

Chapter 1

MRI Basics

A basic understanding of Magnetic Resonance Imaging (MRI) theory is necessary in order to understand the intricacies of RF coil design for traditional and functional MRI imaging. A general introduction MRI theory is provided in this chapter from the viewpoint of classical physics and electromagnetics for readers who are not quite familiar with MRI.

First of all, this chapter deals principally with atomic structure and spin manipulation, which is the physical means of generating signals from the patient for use in imaging. Spin manipulationis explained in a way pertaining to electromagnetic theory. It is also explained how the main magnetic field and the RF field work together in MRI. By the end of this chapter we will have acquired an understanding of the signals which the MRI images are made of as well as the spatial localization method, referred to as frequency encoding and phase encoding. The next chapter will deal with RF coil design and simulation.

1.1 General Introduction to MRI

The basic principles of magnetic resonance imaging (MRI) form the foundation of further understanding this complex subject. It is therefore, important that these ideas are fully grasped before continuing on to RF coil design. There are essentially two ways of explaining the

fundamentals of MRI; classically and via quantum physics. Any discussion requires both and so we have attempted to integrate the two versions.

1.2 Atomic Structure

The atom consists of a central nucleus and orbiting electrons. The nucleus contains nucleons which can be subdivided into protons and neutrons; protons are positively charged. The atomic number is the sum of the protons in the nucleus, and the mass number is the sum of the protons and neutrons in the nucleus. The atom is electrically stable if the number of negatively charged electrons orbiting the nucleus equals the number of positively charged protons in the nucleus. Atoms that are electrically unstable due to a deficit, or an excess number of electrons, are called ions.

The human body mainly consists of water, H2O, a molecule that contains two hydrogen atoms and an oxygen atom. A hydrogen atom consists of a nucleus containing one proton with an electron orbiting the nucleus. Quantum mechanical(QM) theory states that the proton rotates (or spins) around its own axis, and this phenomenon can be simply referred to as spin. The principles of MRI rely on the spinning motion of specific nuclei present in biological tissues. These are known as MR active nuclei. MR active nuclei are characterized by their tendency to align their axis of rotation to an applied external magnetic field. According to the laws of electromagnetic induction, nuclei that have a net charge and are spinning acquire a magnetic moment and are able to align with an external magnetic field. This occurs if the mass number is odd. The process of this interaction is angular momentum or spin.

Important examples of MR active nuclei, together with their mass numbers are listed below:

Hydrogen	1
Carbon	13
Nitrogen	15
Oxygen	17
Fluorine	19
Sodium	23
Phosphorus	31

1.3 Basic Spin Manipulation

A dipole is a separation of two opposite charges, and an example from electrostaticsis the electric dipole, where two opposite charges (monopoles) with equalmagnitude are separated by a distance. A magnetic dipole is defined as an infinitesimally small loop of steady current. Such a magnetic dipole can be characterized by its dipole moment $\vec{m}$ .As shown in Fig. 1.1.

In the absence of an applied magnetic field, the magnetic moments $\vec{m}$ of protons are randomly oriented. The MRI scanner is able to partially align some of the dipole moments $\vec{m}$ of protons in the sample (patient) using a strong static external magnetic field $\overrightarrow{B_0}$. The sum of the dipole moments is no longer a zero-vector, but a vector pointing in the direction of the $\overrightarrow{B_0}$ field called the magnetization vector $\overrightarrow{M}$. This is also known as the net magnetization vector (NMV). Each nucleus that makes up the NMV is spinning on its axis while the influence of $\overrightarrow{B_0}$ field produces an additional spin of the NMV around $\overrightarrow{B_0}$. This secondary spin is called precession and causes the magnetic moments to follow a circular path around $\overrightarrow{B_0}$.

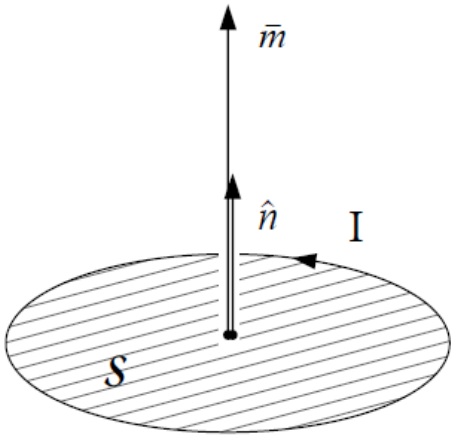

Figure 1.1 Magnetic dipole moment defined as a circular loop current.

The value of the precessional frequency is governed by the Larmorequation. The Larmor equation states that:

The processional frequency $\omega_0 = \omega_0 = B_0 \times \gamma$

Where B_0 is the main magnetic field strength and γ is the gyro-magnetic ratio.

The gyro-magnetic ratio expresses the relationship between the angular momentum and themagnetic moment of each MR active nucleus. It is constant and is expressed as the precessional frequency of a specificMR active nucleus at 1 T. The unit of the gyro-magnetic ratio is therefore MHz/T. The gyro-magnetic ratio of hydrogen is 42.57 MHz/T. Other MR active nuclei have different gyro-magnetic ratios, and therefore have different precessional frequencies at the same field strength. In addition, different nuclei have different precessional frequencies at different field strengths. The precessional frequency is often called the *Larmor frequency*, because it is determined by the Larmor equation. As the gyro-magnetic ratio is a constant of proportionality, B_0 is proportional to the Larmor frequency. Therefore if B_0 increases, the Larmor frequency increases.

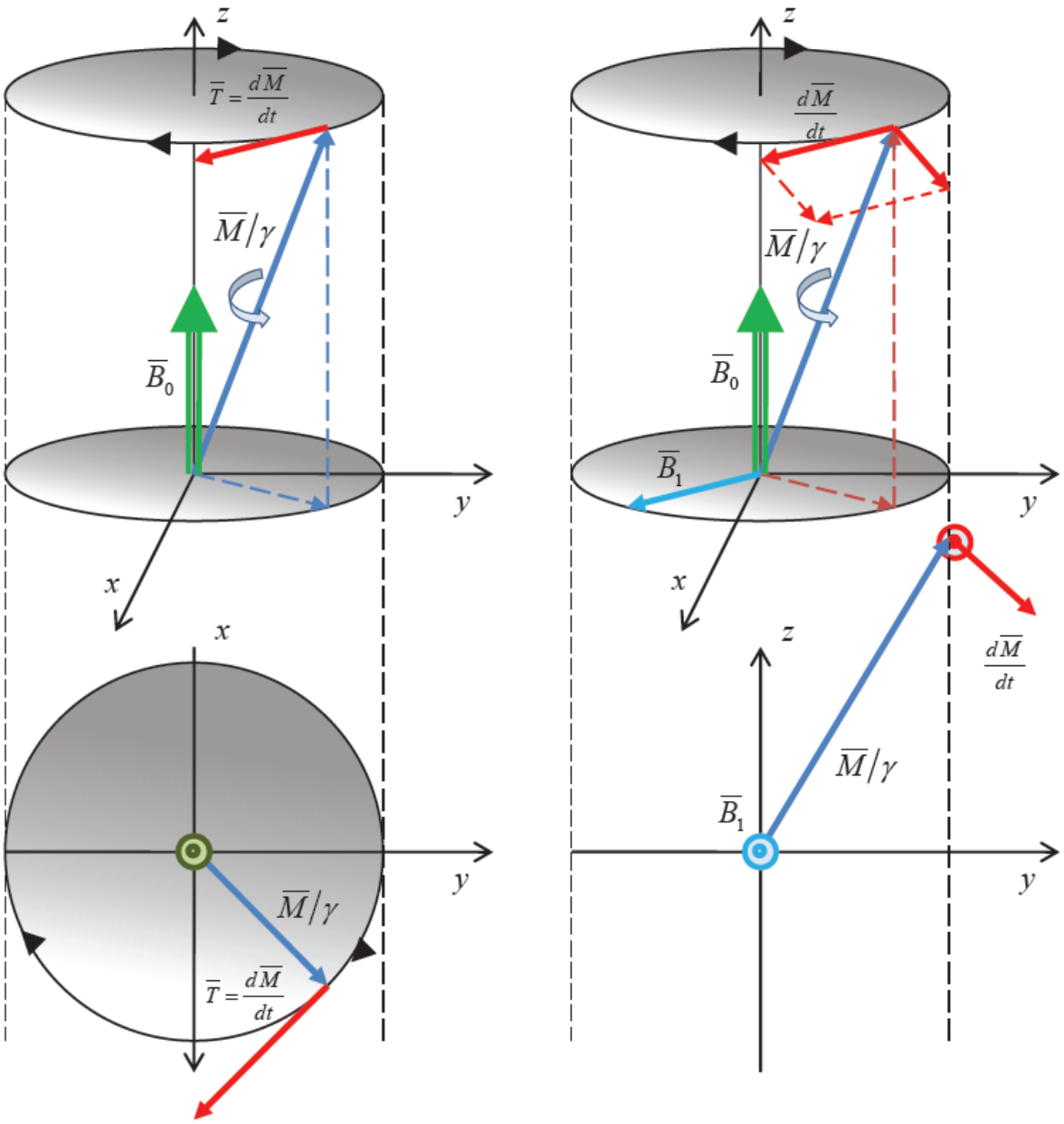

Figure 1.2 Left: Precession around $\overrightarrow{B_0}$. The red torque vector always points tangentially to the circular motion (because it is the cross product of $\overrightarrow{B_0}$ and $\overrightarrow{M}/\gamma$). Right: Precession around $\overrightarrow{B_0}$ and $\overrightarrow{B_1}$ changes the angle of $\overrightarrow{M}$. The precession now occurs around both $\overrightarrow{B_0}$ and $\overrightarrow{B_1}$.

1.3.1 Excitation by RF Field

Now we want to investigate the situation where the patient has entered the scanner, and we assume that the sum of the magnetic dipole moments inside the patienthas come to rest in equilibrium and pointing in the direction of the $\overrightarrow{B_0}$ field. We are now interested in exciting the dipole moments by using an external RF field B_1, the first result is that the NMV moves out of alignment away from B_0 with an angle. This angle is called the flip angle. The second result is that the magnetic moments within the transverse plane move into phase with each other, which means that all the magnetic moments are at the same position on the precessional path at any given time.

As a result, Faraday's laws of induction state that if any conductive loop or a receiver is placed in the area of a moving magnetic field, a voltage is induced in this receiver. Signal is produced when coherent (in phase) magnetization cuts across the coil. Therefore the moving NMV produces magnetic field fluctuations inside the coil. As the NMV precesses at the Larmor frequency in the transverse plane, a voltage is induced in the coil. This voltage constitutes the MR signal. The frequency of the signal is the same as the Larmor frequency.

1.3.2 Relaxation

When the external magnetic field is off, the NMV will tend to relax. During relaxation the NMV gives up the absorbed RF energy and returns to $\overrightarrow{B_0}$. At the same time independently the magnetic moments of the NMV lose transverse magnetization due to dephasing, as shown in Fig.

1.3.

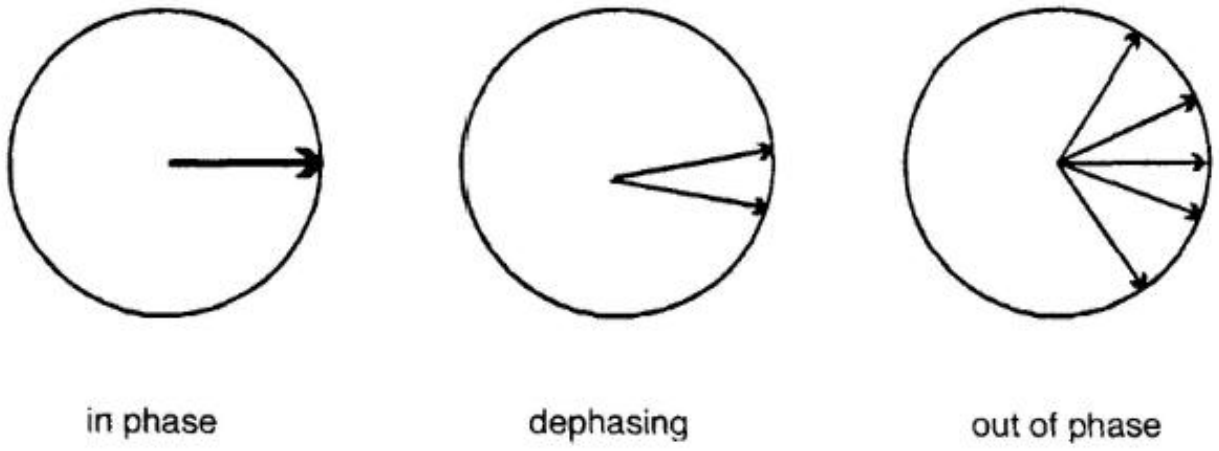

Figure 1.3 Dephasing phenomenon looking down onto the transverse plane

Relaxation results in recovery of magnetization in the longitudinal plane and decay of magnetization in the transverse plane.

- The recovery of longitudinal magnetization is caused by a process termed T1 recovery.
- The decay of transverse magnetization is caused by a process termed T2 decay.

1.4 Signal Detection

The usual way of detecting the precessing magnetization signal is by magnetic induction, which is governed by Faraday's law. Placing a coil near an excited sample will cause the change in flux through the coil to generate a voltage across the terminals of the coil which can be measured. There are many types of coils, but for the purpose of the conceptual understanding of signal reception in MRI, we shall focus on the simplest coil for now.

The simplest coil is called a loop coil. It can be thought of as either a loop antenna or an RF solenoid (inductor) with only one winding. Loop coils are used as surface coils that receive an MR signal in close proximity, whereas avolume coil (such as a birdcage coil) is often used both for excitation and reception of a larger volume. These coils will be treated more in-depth in the following chapters.

1.4.1 Gradients

There are three types of magnetic field existing inside a MRI scanner. The B_0 field generated by the main magnet and the B_1 field generated by RF coils, both of which have been introduced already. The 3rd one is the gradient field generated by gradient coils. This gradient field interacts with the main static magnetic field, so that the magnetic field strength along the axis of the gradient coil is altered in a linear way. The field in the middle of the axis of the gradient remains the same as the main magnetic field. This is called the magnetic isocentre. The magnetic field strength increases relative to isocentre along one direction of the gradient axis,

and decreases along the other direction. The magnitude of B_0 is altered in a linear fashion by the gradient coil, so is the processional frequency experienced by nuclei situated along the axis of the gradient, both of which can be predicted as shown in Fig 1.4 and Fig 1.5.

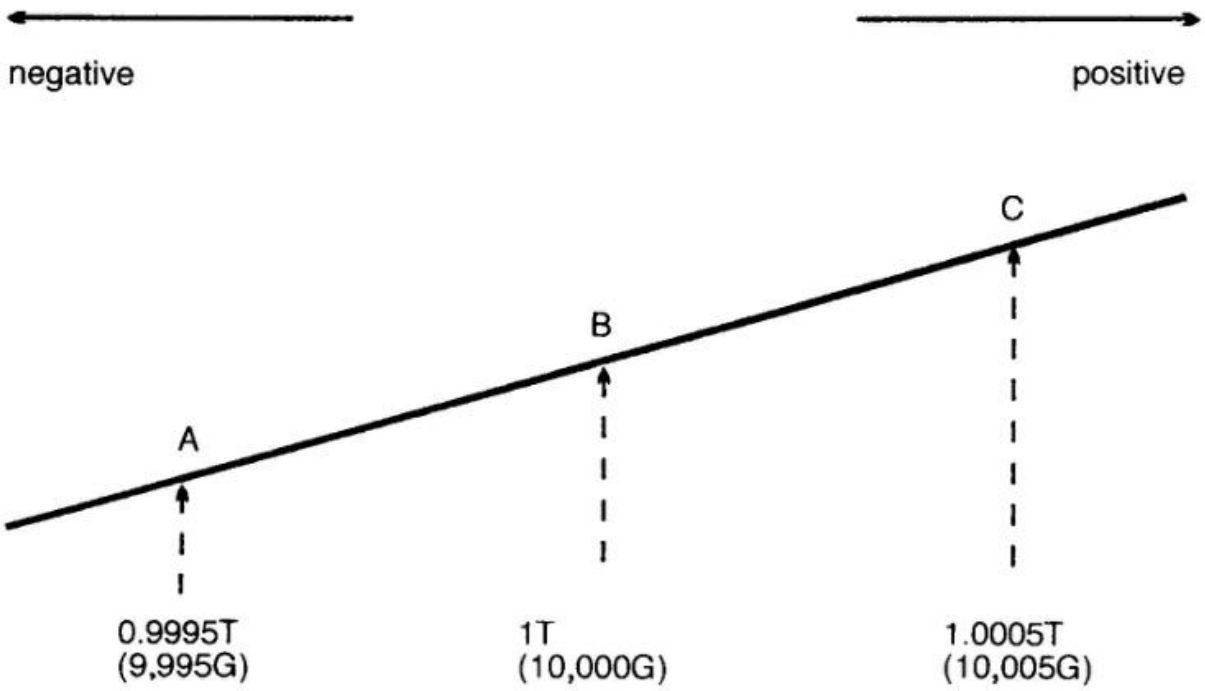

Figure 1.4 The gradients.

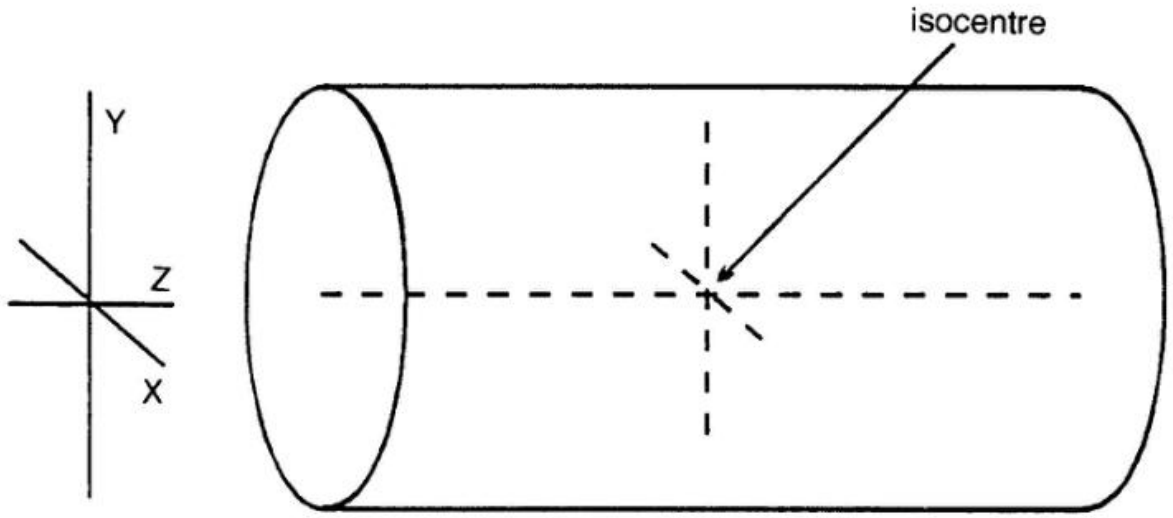

Figure 1.5 The X, Y and Z gradient axes.

1.4.2 Slice selection

As what have been stated previously, when a gradient coil is switched on, the magnetic field strength, and therefore the precessional frequency of nuclei located along its axis, is altered in a linear fashion. As a result, a specific point along the axis of the gradient has a specific precessional frequency. A slice situated at a certainpoint along the axis of the gradient has a particular precessional frequency. A slice can therefore be selectively excited, by transmitting RF energy with a band of frequencies coinciding with the Larmor frequencies within a particular slice as defined by the slice select gradient. Resonance of nuclei within the slice occurs because RF energy with the same frequency is transmitted. However, nuclei situated in other slices along the gradient donot resonate, because their precessional frequency is different due to the presence of the gradient (Fig. 3.4). A specific slice is therefore excited and located within the patient.

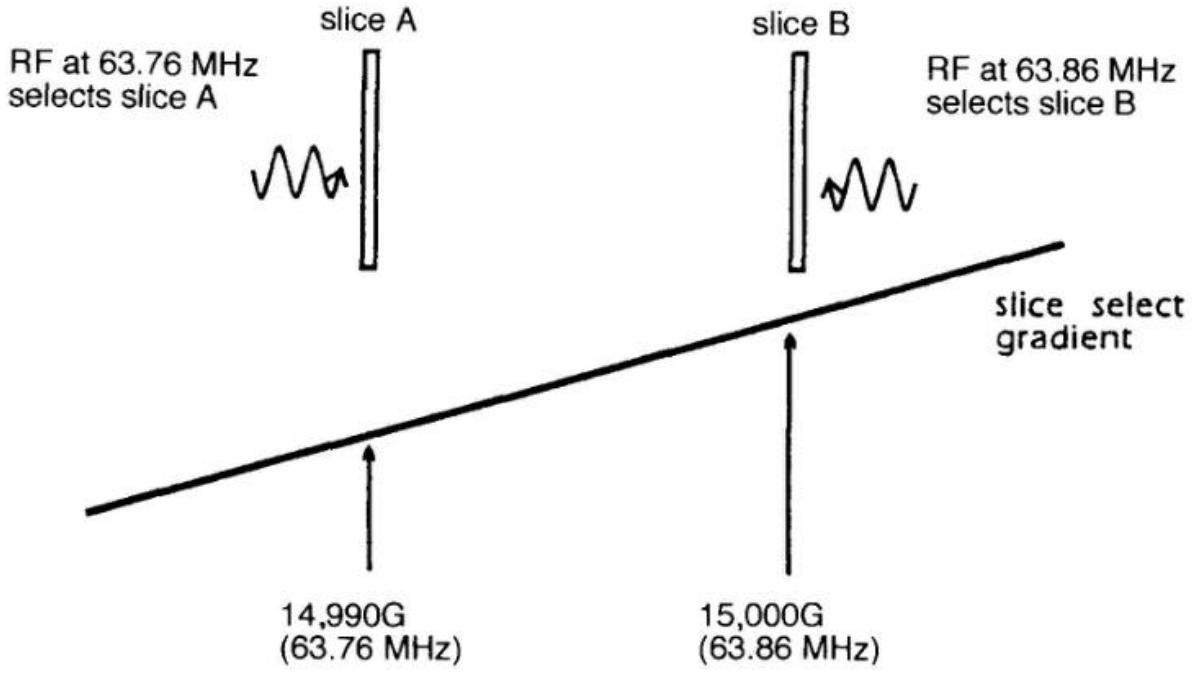

Figure 1.6 Slice selection.

1.4.3 Frequency encoding

Once a slice has been selected, the signal coming from it must be located along the rest of both axes of the image. The signal is usually located along the long axis of the anatomy by a process known as frequency encoding. When the frequency encoding gradient is switched on, the magnetic field strength and therefore the precessional frequency of signal along the axis of the gradient, is altered in a linear fashion. The gradient therefore produces afrequency difference or shift of signal along its axis. The signal can now belocated along the axis of the gradient according to its frequency (Fig. 1.7).

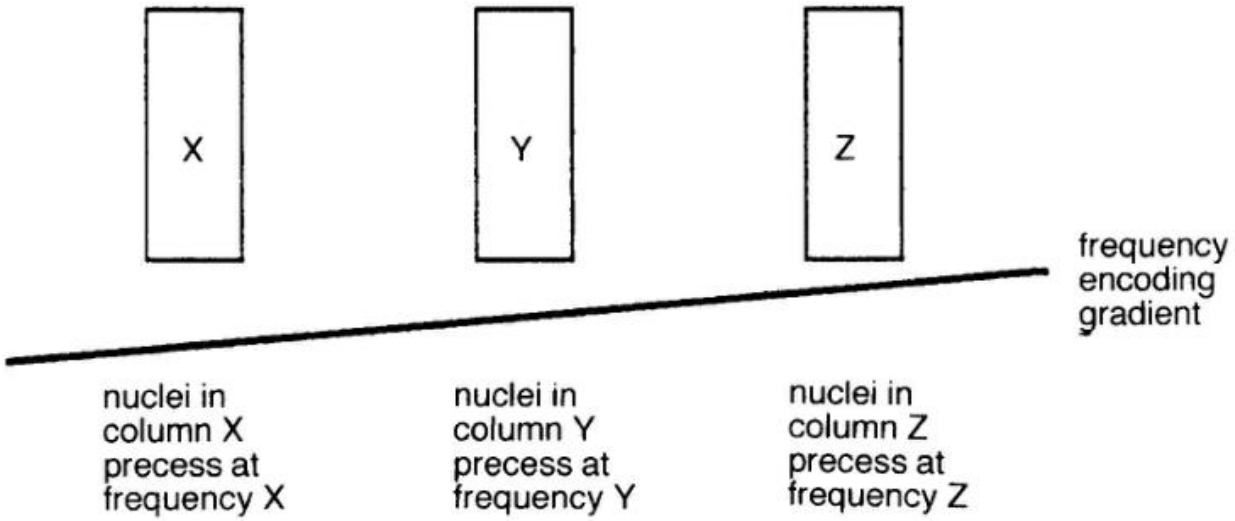

Figure 1.7 Frequency shift

1.4.4 Phase encoding

Signal must now be located along the remaining axis of the image and this localization of signal is called phase encoding. When the phase encoding gradient is switched on, the magnetic field strength and therefore theprecessional frequency of nuclei along the axis of the gradient is

altered. As the speed of precession of the nuclei changes, so does the accumulated phase of the magnetic moments along the precessional path. Nuclei which have sped up due to the presence of the gradient move further around their precessional path than if the gradient had not been applied while nuclei that have allowed down due to presence of the gradient move further back (Fig.1.8).

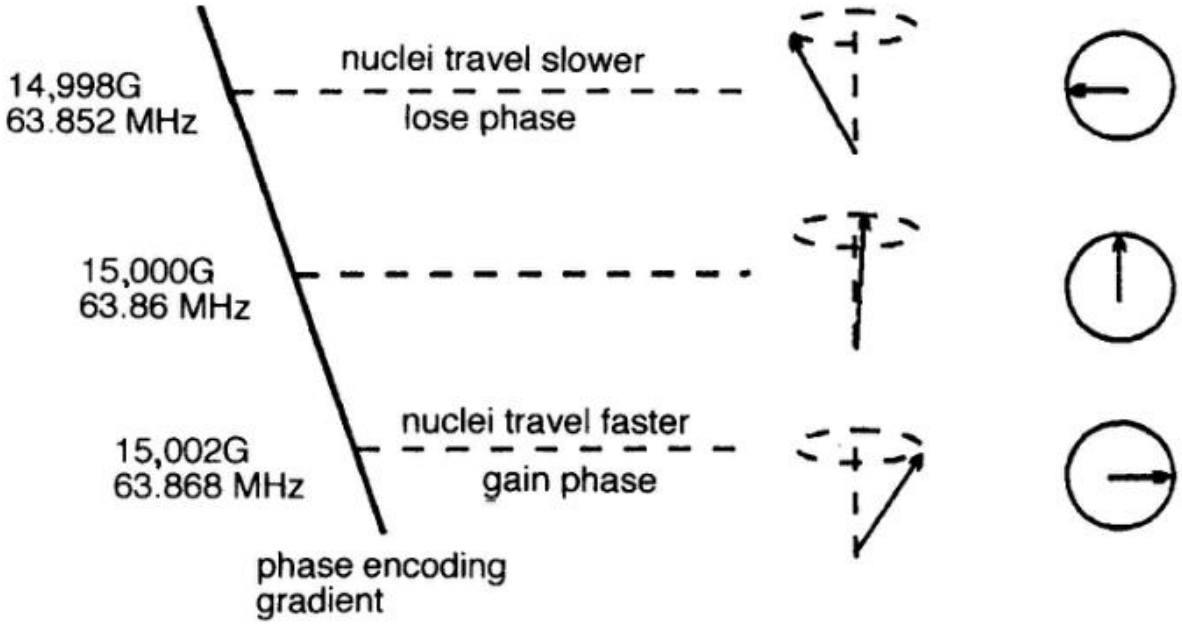

Figure 1.8 Phase encoding

There is now a phase difference or shift between nuclei positioned alongthe axis of the gradient. When the phase encoding gradient is switched off, the magnetic field strength experienced by the nuclei returns to the main field strength B_0 , therefore the precessional frequency of all the nuclei returns to the Larmor frequency. However, the phase difference between the nuclei remains. The nuclei travel at the same speed around their precessional paths, but their phases or positions on the clock are different. This difference in phase between the nuclei is used to determine their position along the phase encoding gradient.

1.4.5 Fast Fourier Transform (FFT)

The acquired data held now needs to be converted into an image. This conversion is made mathematically by a process known as *Fast Fourier Transform (FFT).* The signal measured as a relationship of its frequency against time. The FFT process mathematically converts this to calculate the amplitude of individual frequencies. The signal intensity in time domain is therefore converted to a signal intensity in frequency domain. As the FFT process deals in frequencies, the system must acquire both phase and frequency shifts in frequencies (Fig. 1.9). This is why it is necessary to convert the phase shift produced as a result of the application of each of the phase gradients into a frequency.

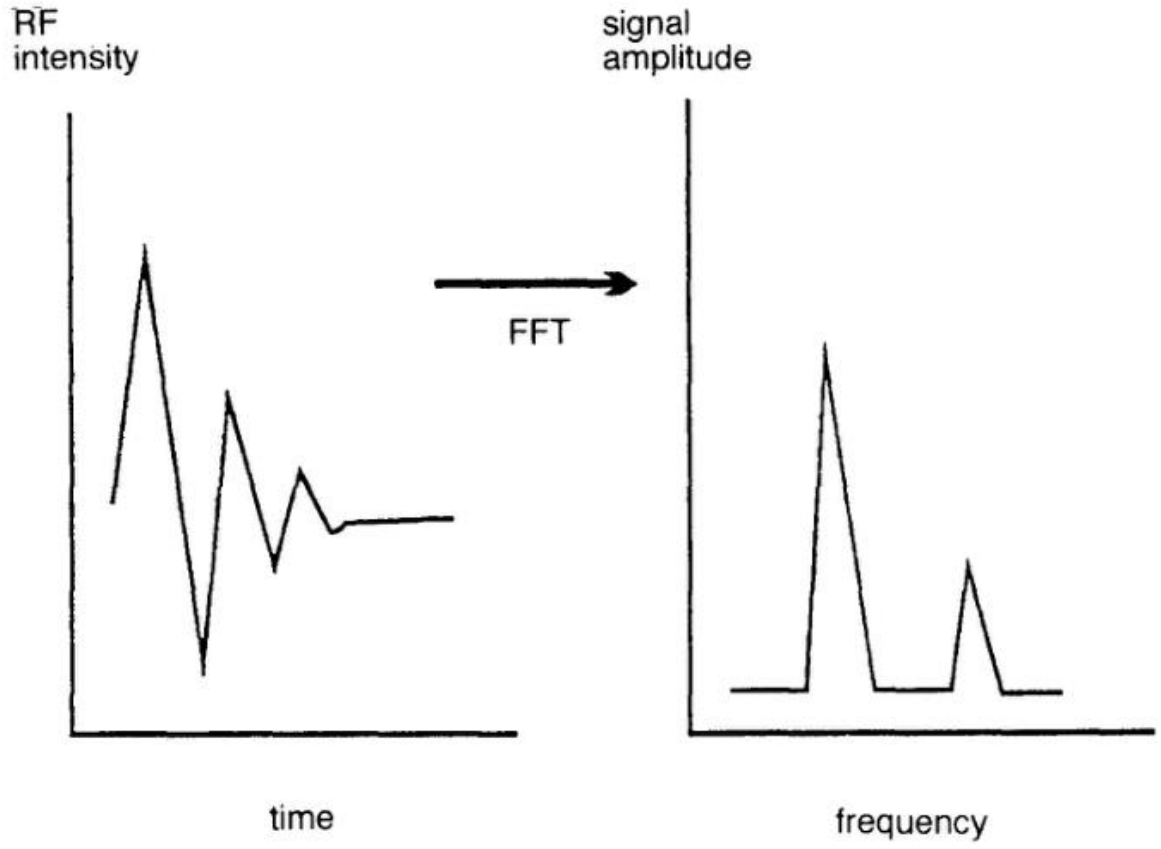

Figure 1.9 the Fast Fourier Transform

1.5 Summary

It is important to understand the basic principles of the electromagnetics of MRI in order to design coils. When a patient or sample is inserted into theMRI scanner, the NMV will be aligned in the direction of the main magnetic field. The role of the transmission coil is to tip tis magnetization to the transversal plane. The magnetization will rotate (precess) transversally, and the flux from the magnetization induces a voltage in the receive coil. The same coil can be used for transmission and reception, or two separate coils can be used. The geometric positioning with respect to the precessing magnetization is important in order to receive as much flux as possible. When the magnetization is restored to its equilibrium direction along the main magnetic field, no signal is induced in the coil. This chapter has also introduced the basic mechanisms of gradients, how signal is determined in all three dimensions and how data is acquired and converted into an MRI image. Next chapter will be focused more detailed on RF coil design.

Chapter 2

Coil Design and Simulation

In all NMR, it is necessary to excite the nuclei into coherent precession. This requires coupling between the nuclei and the transmitter. To receive a meaningful signal, one also needs a device to couple the nuclei to the receiver. The devices which serve both of the two functions are called RF coils.

In human imaging, the wavelength is generally the same order of magnitude as the sample. To build an effective coil in this case is very difficult. Traditionally saddle coils have been preferred over solenoids as they allow better patient access when the main magnet is also of a solenoidal shape. Increasingly, however, a design called the birdcage coil is being used and preferred. This type of coil cleverly combines lumped capacitors with distributed "leg" inductance to form a volume resonator. The resonance increases the efficiency of the coil at operating frequencies.

It is very important that the coil generates a very uniform B_1 magnetic field, since the flip angle is a function of field magnitude. Also a very high Signal to noise ratio (SNR) is desired for reception. Unfortunately, the requirement for a uniform field distribution and a high SNR are fundamentally in direct conflict and cannot usually be achieved simultaneously, so a trade-off is

always necessary. One approach to resolving this conflict is to use one RF coil for transmitting and the other for receiving while this will make it even more complicated to design and build. In our case, a birdcage coil is used for both transmit and receive. Since this coil is placed fairly close to the phantom, a good SNR should be acquired as will be proved by the MRI image in Chapter 4.

It is also desirable to have a coil which permits “quadrature” excitation and detection. Electromagnetically this is equivalent to being able to generate and receive circularly polarized fields. For this, a circuit is needed to split equally the transmitting power into two channels and introduce a 90 degree phase delay in one of the channels. These two channels are then fed to the two inputs of the RF coil to produce two fields perpendicular to each other. For receiving, the same principle can be applied and this will be talked about in the next chapter.

2.1 Introduction

The first birdcage coil was designed and fabricated by Hayes and it was a high-pass coil which produced a linearly polarized field. On the other hand, a quadrature coil produces a circularly polarized field and is preferred over a linear one since itimproves the SNR by a factor of $\sqrt{2}$ and also the RF transmission efficiency. A circularly polarized field implies that the two orthogonal resonant modes are at the same frequency; one mode carries current proportional to sine of the cylindrical azimuthal angle and the other mode carries current proportional to the cosine of that angle.

In the design of a birdcage coil, a RF shield is necessary to reduce the interaction between the RF coil and the gradient or the shim coils. These interactions degrade the performance of the RF coilin SNR and in MR images. Moreover, it provides a stable environment for tuning and matching. At high fields the radiation losses are very high. A shielded coil will also make sure that all the energy is within the coil. Thus, it is necessary to completely overlap the shield and coil. Normally, the diameter of the shield should be 1.5 times that of the coil and the length the coil should be 60% that of the shield.

It is the objective of this thesis to present a 2-port drive birdcage coil. The coil dimensions have to be chosen after taking into consideration the effect on SNR, homogeneity and manufacture issues. Next, strategies for tuning, matching and decoupling the 2 excited ports are presented. Detailed description and results are given on bench testing and MRI images are taken to evaluate performance of the coil. At last, the reader is made aware of various issues encountered during the fabrication of this coil and suggestions are given on the future coil design.

2.2 Theory of Birdcage Coils

RF coils are used for transmitting RF pulses and for receive. Specifically, the coil generates RF pulses at the Larmor frequency to excite the nuclei in the object which is going to be imaged. When the RF excitation pulse is off, the nuclei will relax; during relaxation the nuclei will emit RF energy at Larmor frequency. This energy will be received by the RF coil. The birdcage coil is a volume coil and is an example of a RF coil. Surface coils are also an example of RF coils. Volume coils are preferred over surface coils because volume coils are able to

produce a homogenous B1 field in the volume of interest as compared to surface coils so that the nuclei can be uniformly excited. Surface coils have the advantages that they are small and can be made of various shapes to fit the contour of the object to be imaged. Thus the SNR of the surface coil is usually higher than the volume coil, since the surface coil is in close proximity to the sample. But, the disadvantage of surface coils is that the sensitivity falls off quickly. In other words, surface coils have a low penetration depth as compared to volume coils.

The birdcage coil is made of multiple parallel conductive segments that are parallel to the z axis (Fig 2.1). These parallel conductive segments are referred to as the rungs or the legs. These rungs interconnect a pair of conductive loop segments, the two top and bottom loops are called the end rings or the rings. A high-pass coil is where the conductive loops have capacitors between adjacent rungs. A low-pass coil is where the capacitors are in the middle of the rungs. A hybrid coil is where the capacitors are located on the loop segments and the rungs. A high-pass is so called because the high frequency signals will tend to pass through capacitive elements while low frequency signals will tend to pass through inductive elements.

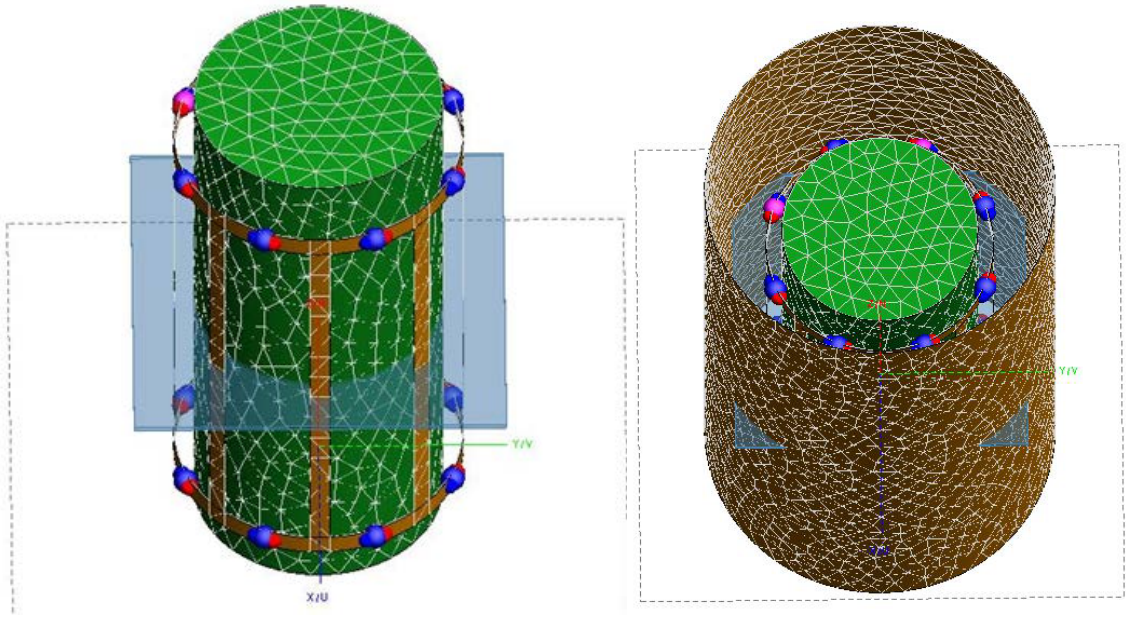

Figure 2.1 1) Left: A high-pass birdcage coil with a phantom put inside. 2) Right: With a RF shield put outside

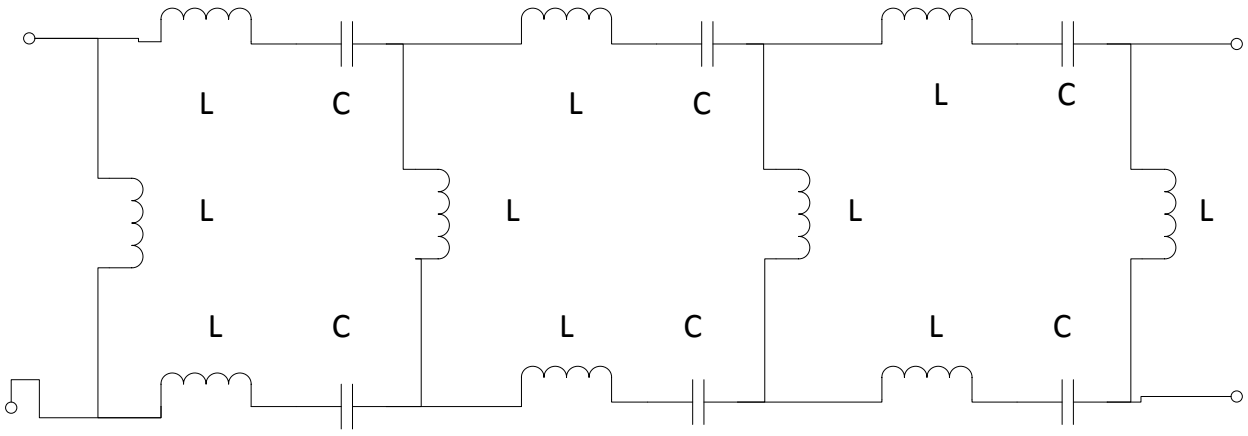

Figure 2.2 Lumped element equivalent circuit of a high-pass birdcage coil

When the coil is fed at a particular location it creates N/2+1 resonant modes; where N is the number of legs. Applying Kirchhoff's voltage law, we get

$$\left(\frac{1}{\omega^2 C} - M\right)\left(I_{J+1} + I_{J-1}\right) - 2\left(\frac{1}{\omega^2 C} - L - M\right) I_J = 0;\ \text{J = 0, 1, 2,.. N}$$

Because of the cylindrical symmetry, the current I_J must satisfy the periodic condition

$$I_J = I_{J+N}$$

Therefore, the N linearly independent solutions have the form as

$$\left(I_J\right)_m = \cos\frac{2\pi mJ}{N};\ \text{m = 0, 1, 2, .. N/2}$$

$$= \sin\frac{2\pi mJ}{N};\ \text{m = 0, 1, 2, .. N/2-1}$$

Where $\left(I_J\right)_m$ denotes the value of the current in the J*th* leg for the m*th*solution.

If we substitute this solution back into the first equation, we are able to get the equation for the resonant frequencies

$$\omega_m = \left[C(M + L/\left(2\sin^2\frac{\pi m}{N}\right)\right]^{-\frac{1}{2}}\quad \text{m = 0, 1, 2, .. N/2}$$

In this equation m=1 generates currents in the straight segments proportional to sinθ which, in turn, produce a homogeneous B1 field. And this is called the dominant mode. For higher order resonant modes, the homogeneity decreases as m increases.

2.3 Simulation

In our design, the dimensions of this birdcage coil were mainly determined by the phantom size and manufacturing issues, given the special structure of this 4.7T MRI scanner in UAB for monkey head imaging (Fig. 2.3), although the effects of SNR and homogeneity were also taken into consideration.

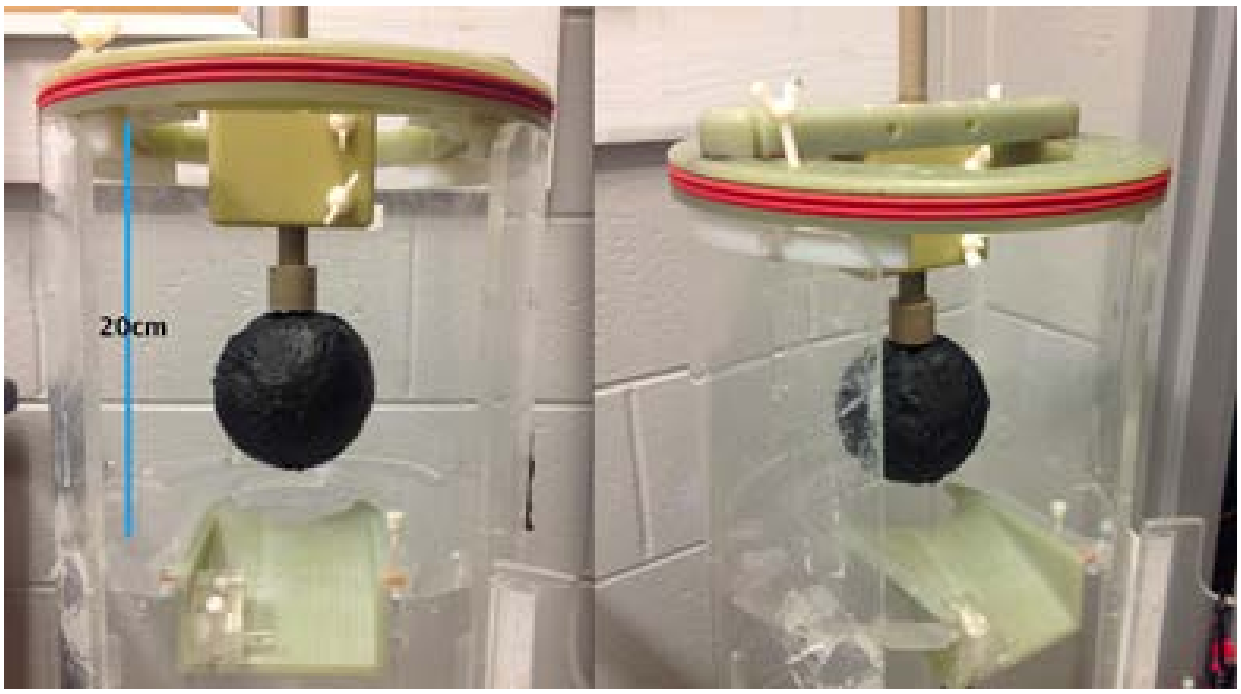

Figure 2.3 Structure of the cylinder goes inside the 4.7T MRI scanner

First of all, we used a former monkey head image to roughly calculate the dimension a monkey head or the phantom to be imaged (Fig. 2.4). And then the dimensions of the coil and RF shield were determined. Trade-offs were made between SNR and homogeneity. Furthermore, the diameter of the RF shield was constrainedby that of the cylinder. So if the RF shield was far away from the coil, it would not fit inside this cylinder.

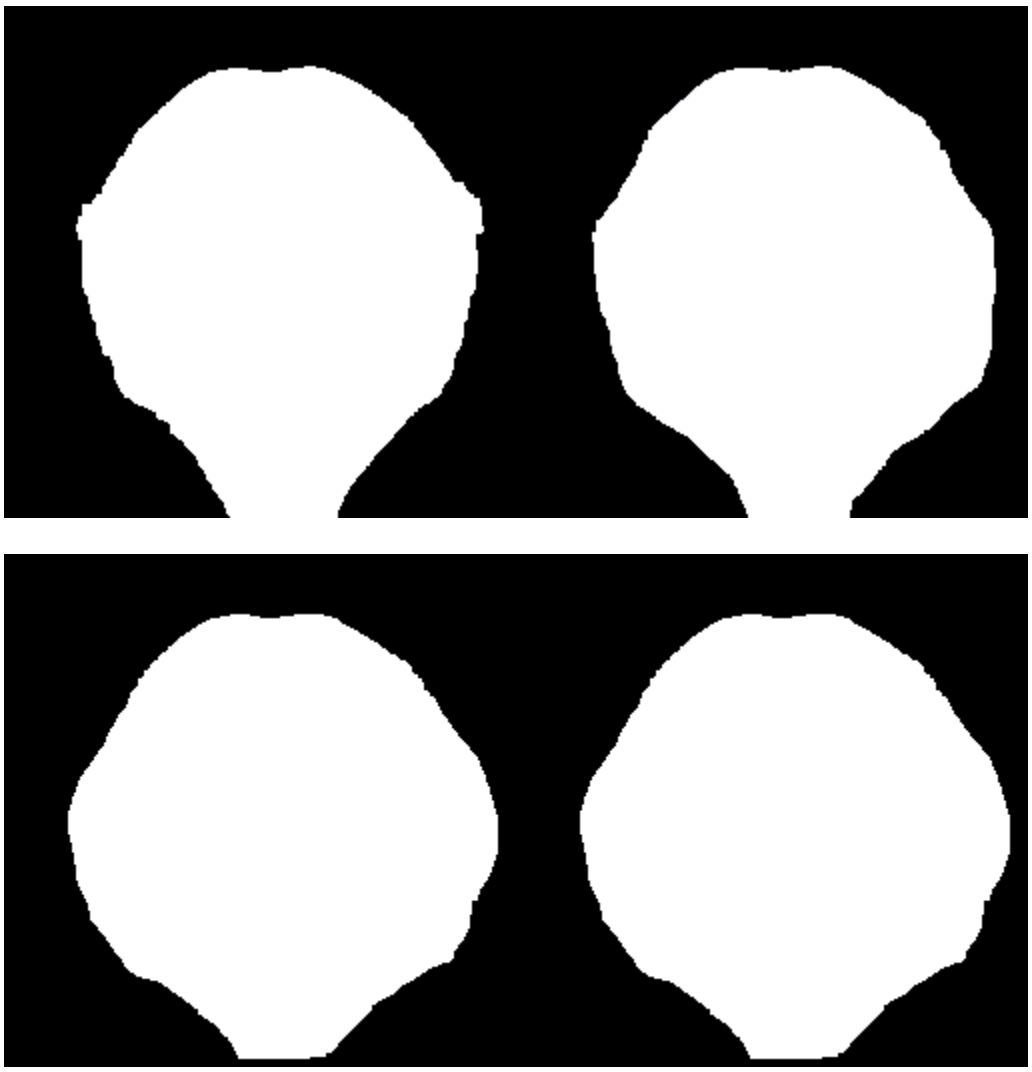

Figure 2.4 A set of monkey head images with different values in z direction.

Once the dimensions were decided, the models of the coil frame, shield and phantom were drawn in the simulation software FEKO (Fig 2.5 & 2.6). After that, the 4-ch birdcage coil together with the RF shield is modeled and simulated using a saline water ball to mimic the physiological constitution of a monkey head (Fig. 2.7).

.

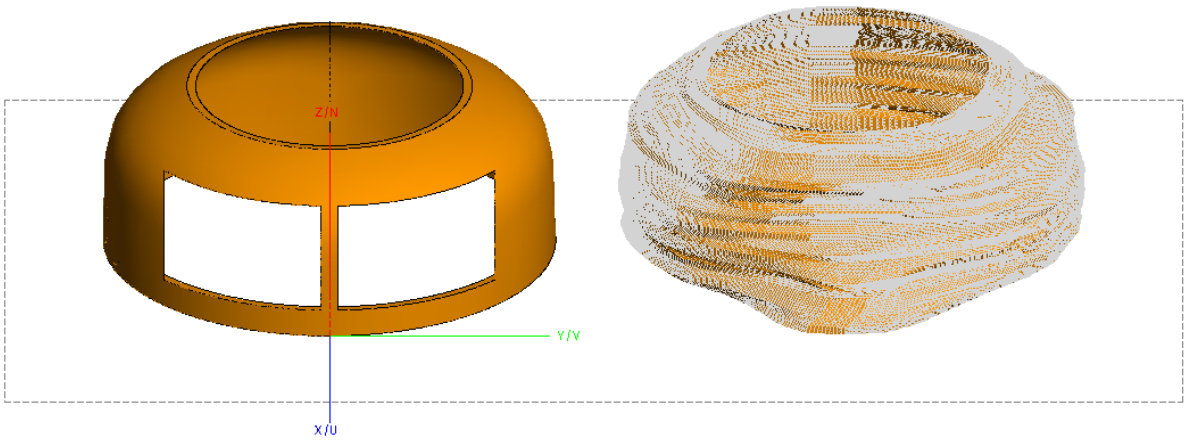

Figure 2.5 A comparison of the coil frame and the monkey head in FEKO.

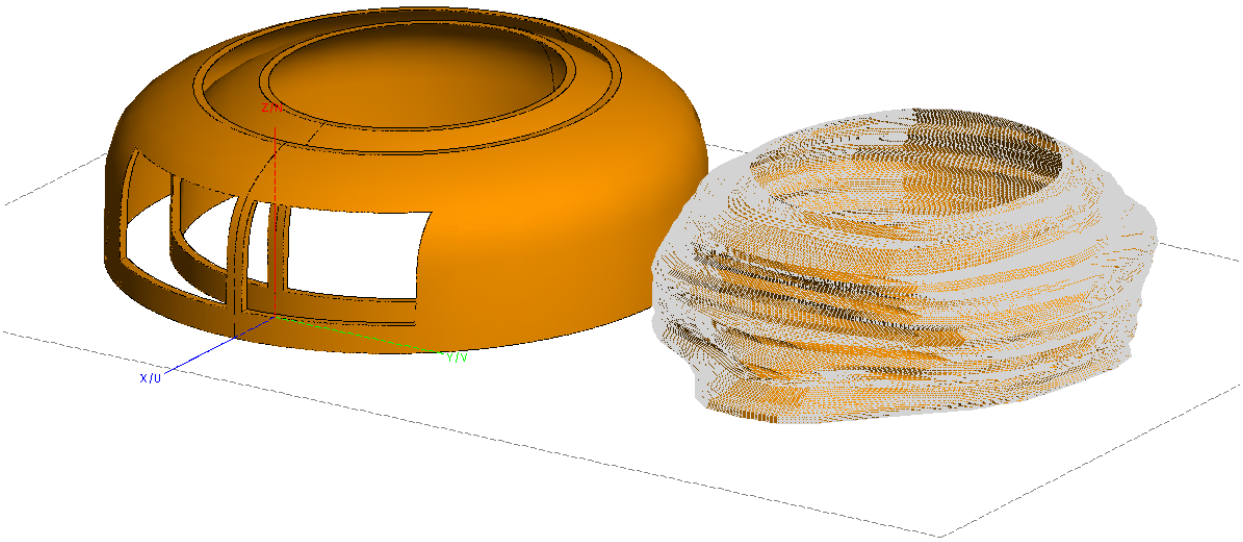

Figure 2.6 A comparison of the coil frame, the shield and the monkey head in FEKO.

In the following section; a brief description is given on the modeled coil, the method used to find the dominant mode and the result B1 field images. A model of the coil, shield and phantom was created in FEKO. An important consideration is how to specify the grid size. Different grid size leads to different time taken by the software to generate a frequency spectrumand B1 field distribution. The grids used in FEKO are small triangles, which are defined

by the triangle edge length. Normally for a MRI RF coil with copper strip, 3 triangles along the cross edge are fine enough. However in this case, we were using copper wires instead in this project. Then the length and diameter of the wire need to be set up in order to define a grid. Since the diameter of the copper wire was already decided(AWG 16), only the length was left to be chosen. I found it the value of the length to be 8mm that we would be able to achieve a good balance between speed and preciseness.

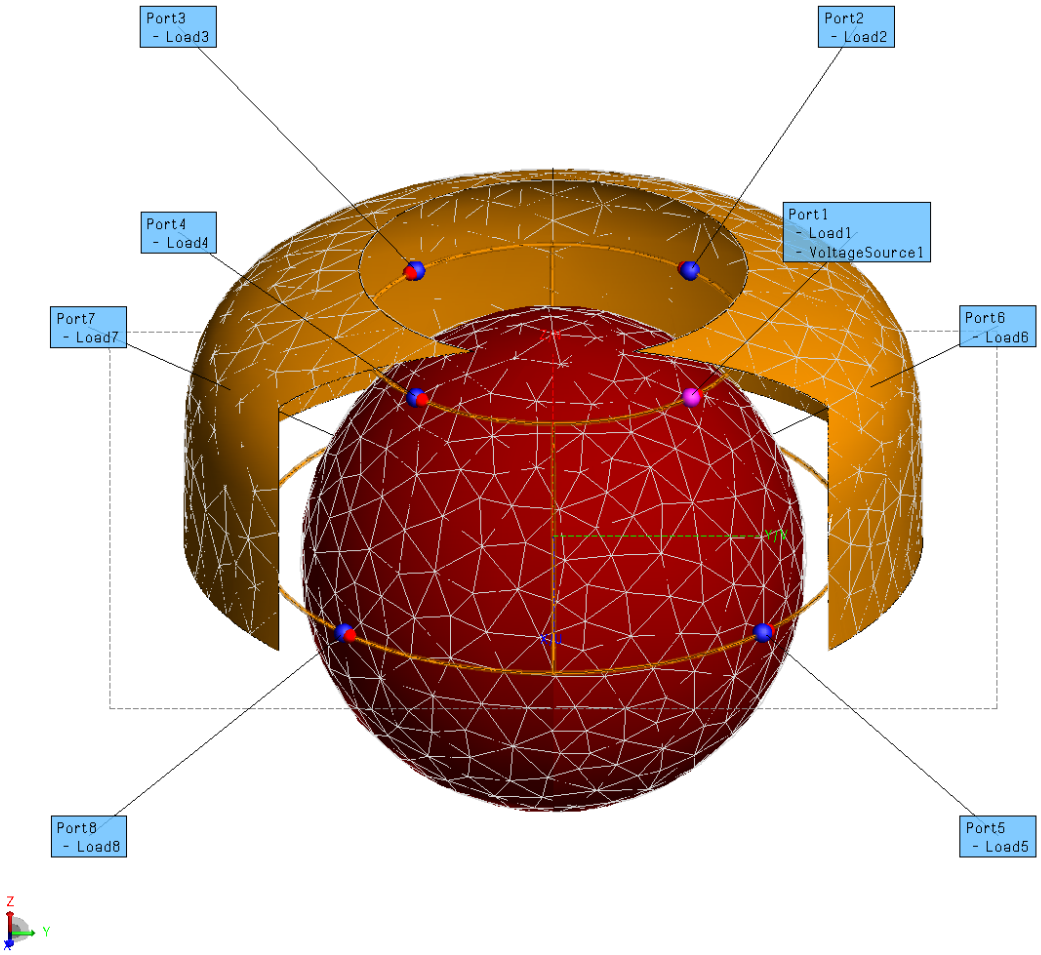

Figure 2.7 Birdcage Coil modeled in FEKO with RF shield and phantom.

Second, a frequency spectrum with reflection coefficient was achieved with a certain capacitor value (Fig 2.8). In theory we know that there will be (N+1)/2 modes where N is the number of the legs. In this case N=4 gives 3 modes in all. The dominate mode was found by tuning each mode to the desired frequency and checking the field distribution since only the dominate mode generates a homogeneous magnetic field at the center of the coil. The field distribution from different cutting planes was achieved (Fig 2.9 & Fig 2.10).

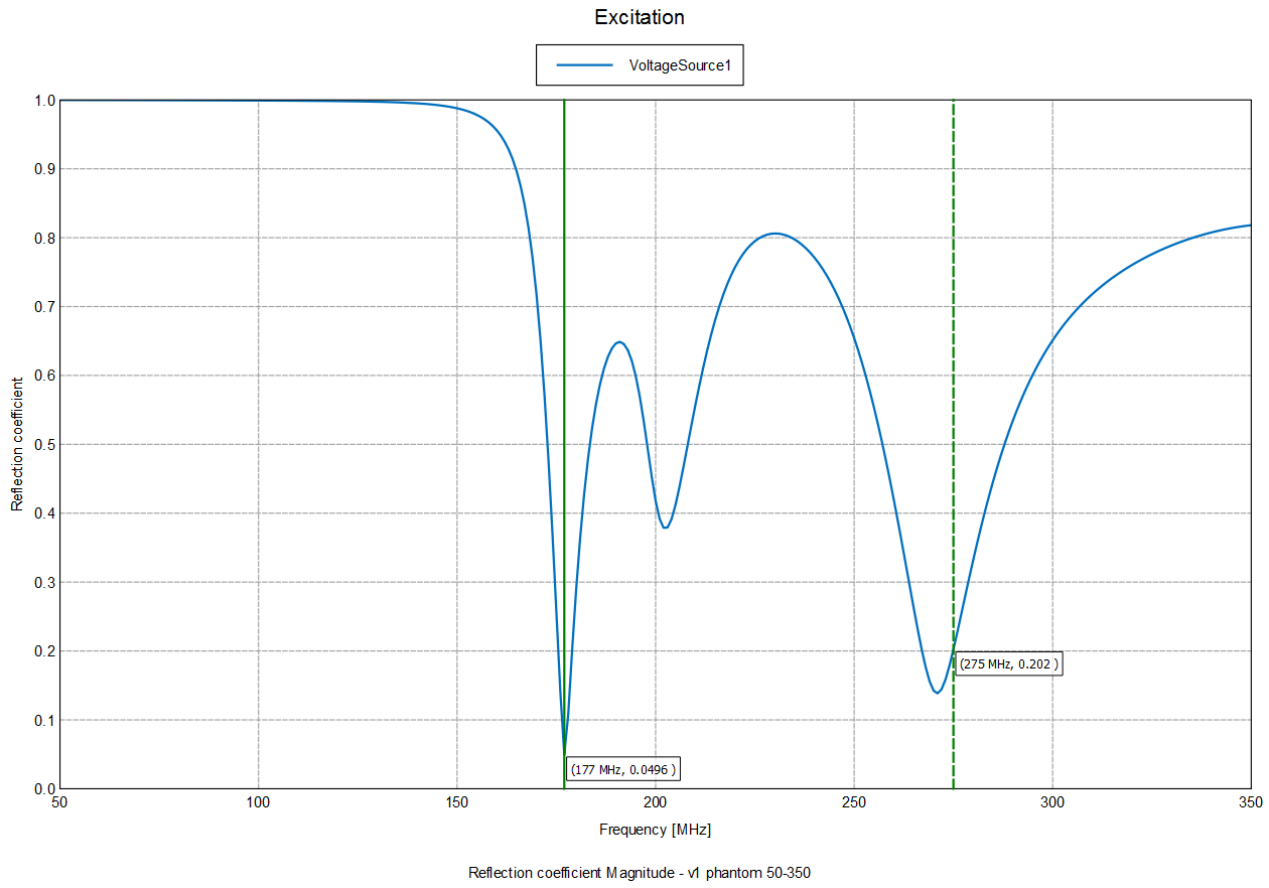

Figure 2.8 The frequency spectrum of reflection coefficient.

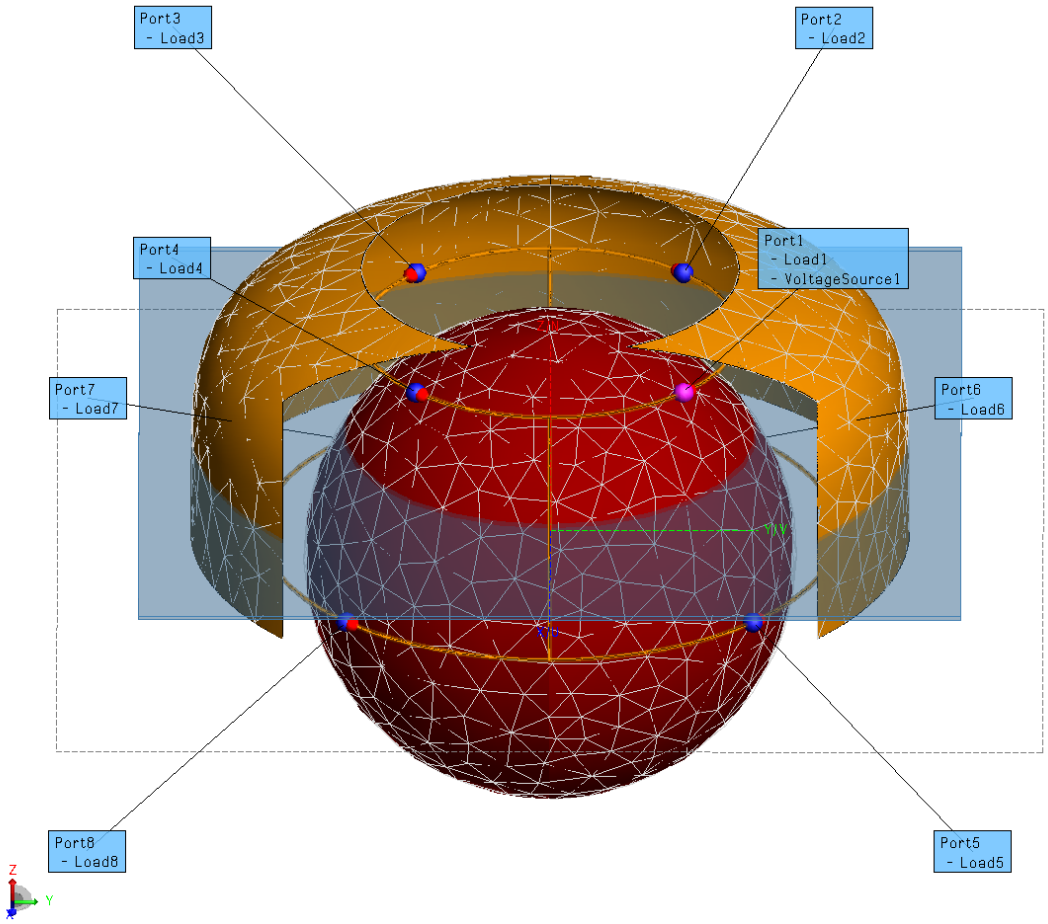
Port3
- Load3
Port2
- Load2
Port4
- Load4
Port1
- Load1
- VoltageSource1
Port7
- Load7
Port6
- Load6
Port8
- Load8
Port5
- Load5
Z
Y

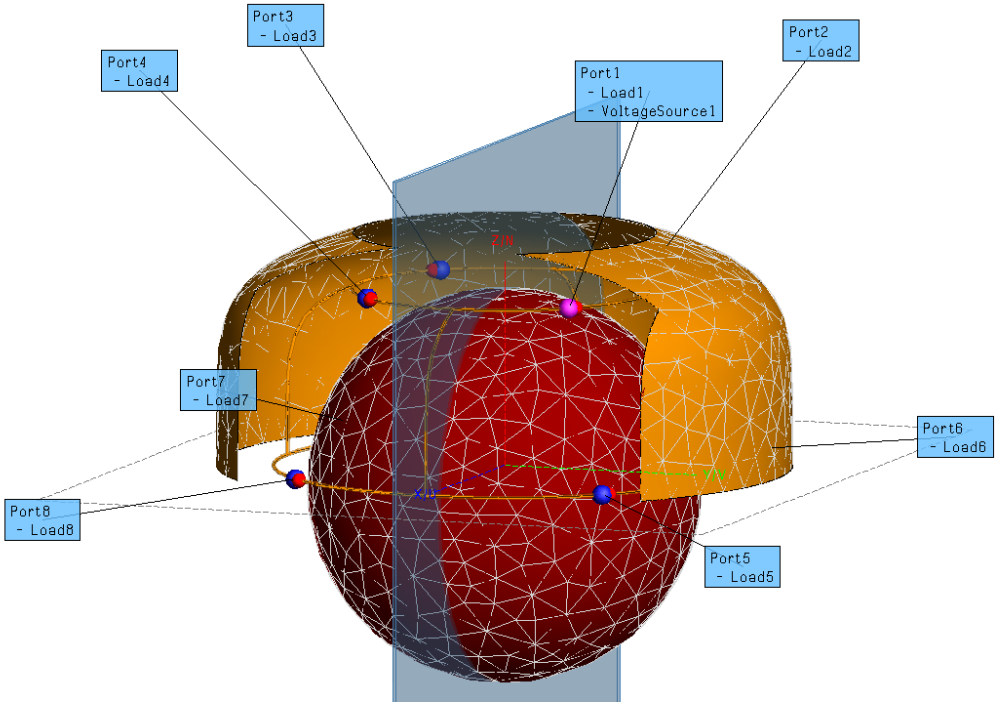
Port3
- Load3
Port2
- Load2
Port4
- Load4
Port1
- Load1
- VoltageSource1
Port7
- Load7
Port6
- Load6
Port8
- Load8
Port5
- Load5

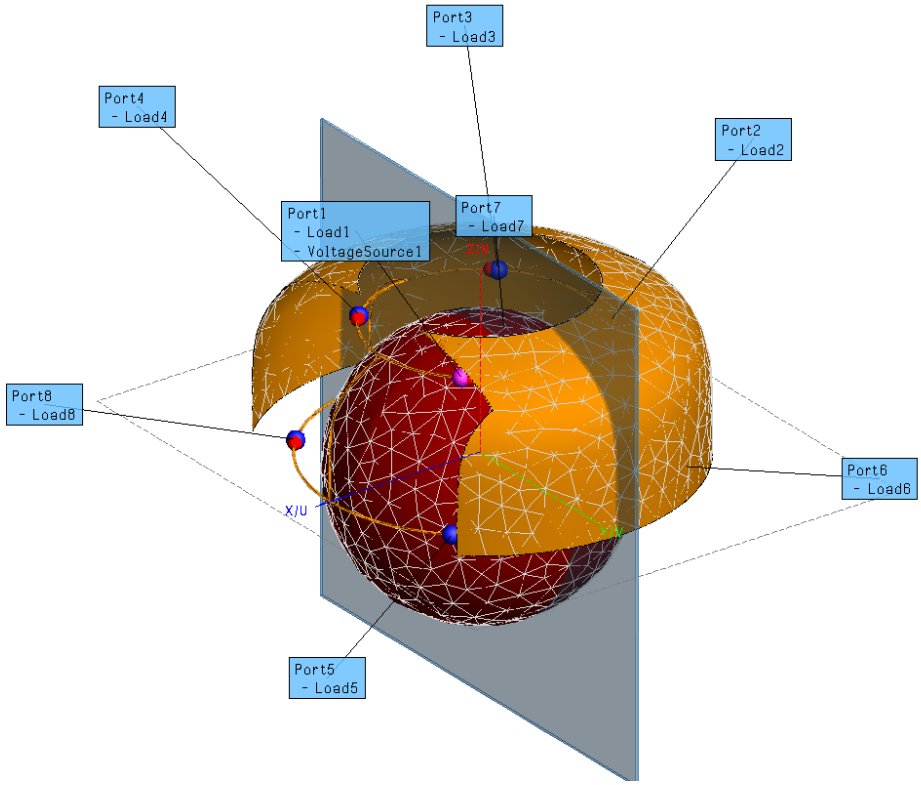

Figure 2.9 Different cutting planes. 1) Top: transverse plane. 2) Middle: sagittal plane. 3) Bottom: coronal plane.

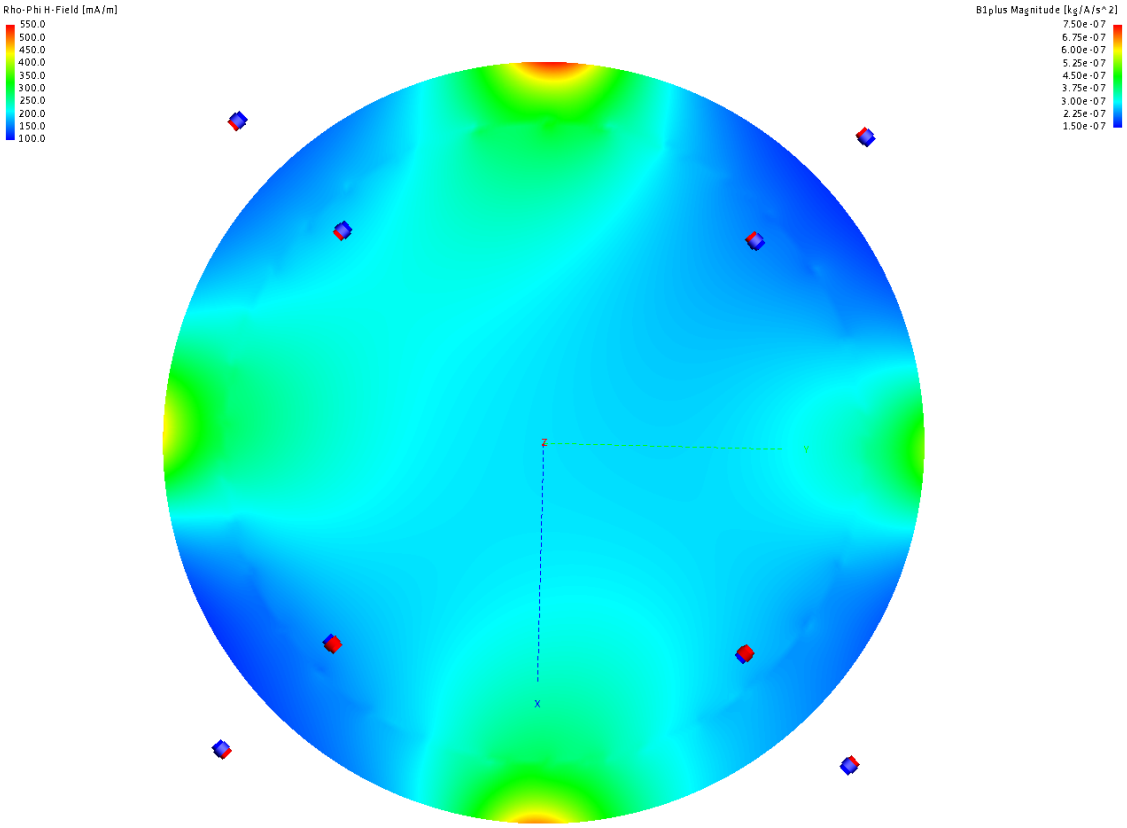
Rho-Phi H-Field [mA/m]
550.0
500.0
450.0
400.0
350.0
300.0
250.0
200.0
150.0
100.0
B1plus Magnitude [kg/A/s^2]
7.50e-07
6.75e-07
6.00e-07
5.25e-07
4.50e-07
3.75e-07
3.00e-07
2.25e-07
1.50e-07
z
y
x

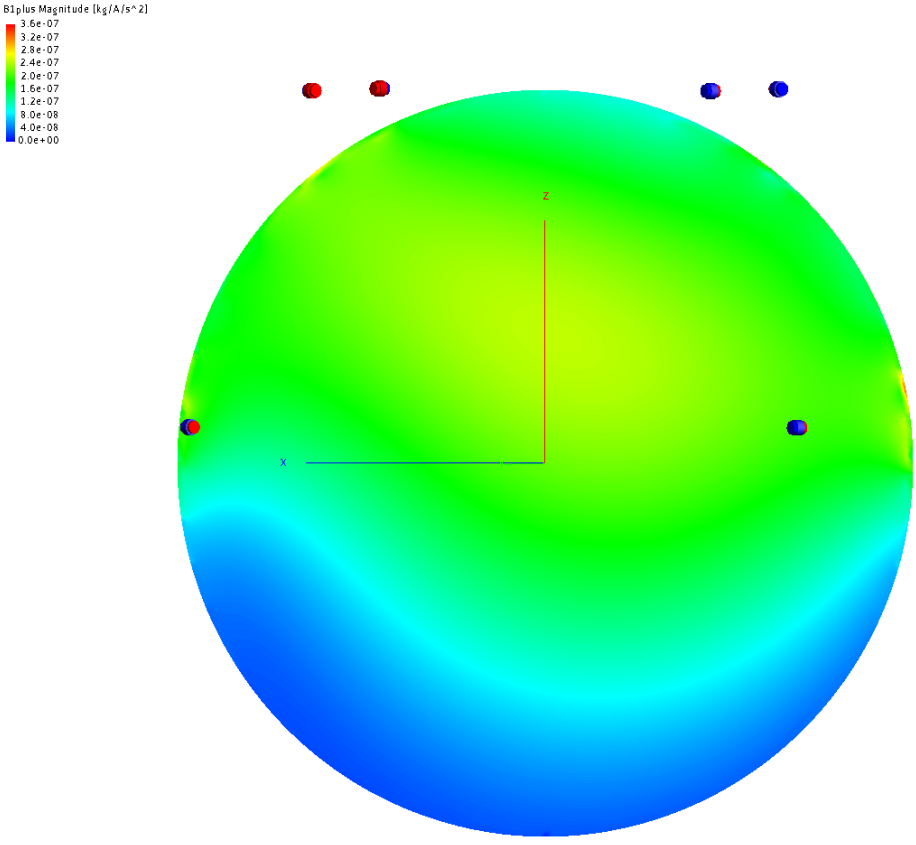
B1plus Magnitude [kg/A/s^2]
3.6e-07
3.2e-07
2.8e-07
2.4e-07
2.0e-07
1.6e-07
1.2e-07
8.0e-08
4.0e-08
0.0e+00
z
x

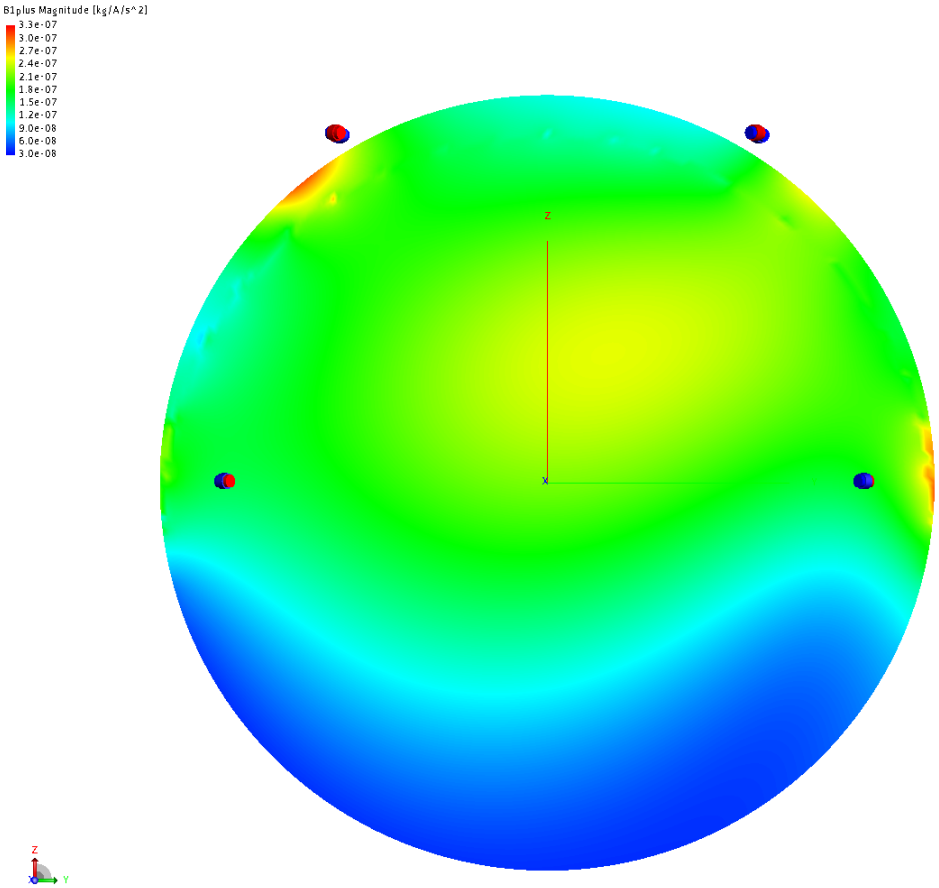

Figure 2.10 B1 field distribution. 1) Top: transverse plane. 2) Middle: sagittal plane. 3) Bottom: coronal plane.

Lastly, the coil and shield frame were designed in FEKO (Fig. 2.11). The coil frame is specially design in following two ways: 1.)Several grooves were added to place to the front end circuit board behind the coil (this will be talked about in the next chapter); 2.) Two “arms” were added on the sides of the coil in order to hold the cross bar as has been shown in the previous figures to make this coil stable during MRI scans.

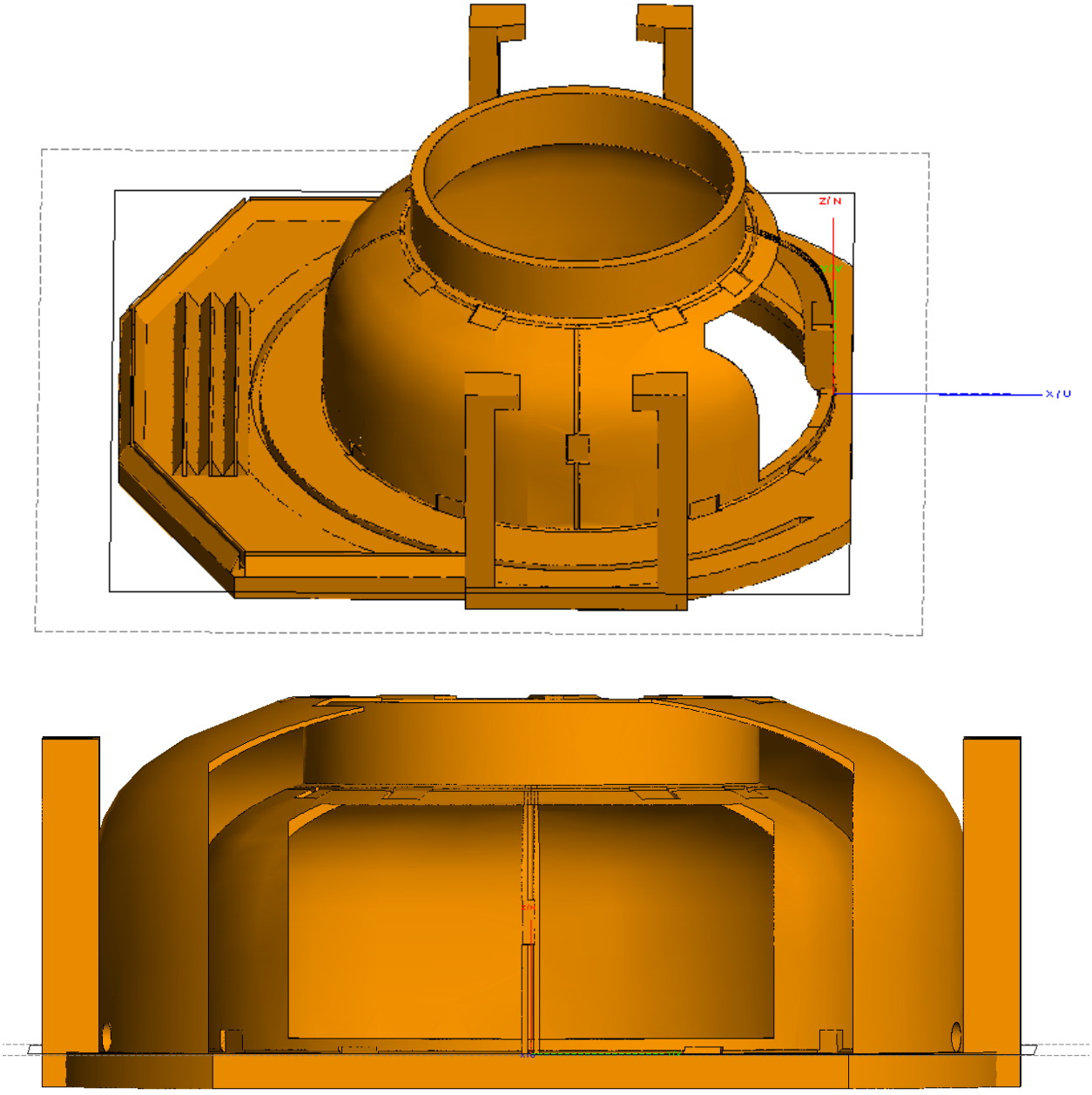

Figure 2.11 Coil frame modeled in FEKO. 1) Top: Coil frame only. 2) Bottom: Coil and shield frame

Chapter 3

Front end Circuit Design

The RF front end is generally defined as everything between the coil and the system. For this 4.7T birdcage transceiver system, the RF front end basically consists of:

- Hybrid
- transmit-receive switch (TR Switch)
- Low noise preamplifier (LNA)

These will be discussed in theory, design and testing results in the following section.

3.1 Hybrid

3.1.1 Introduction

A hybrid coupler is a passive device used in radio and telecommunications. It is a type of directional coupler where the input power is equally divided into the two output ports. The common circuit symbols for a four-port coupler are in Figure 3.1. A coupler will transmit a portion of its power from its input to its through port (port2). The other portion of the power will go to the coupled port (port 3), and ideally none will be received at the isolated port (port 4). If the isolated port is internally terminated in a matched load, the coupler is most often referred to as a directional coupler. If the power split ratio equals to 1:1, which means the power goes to port 2 is the same as that goes to port 3, then this device is the so called a hybrid coupler.

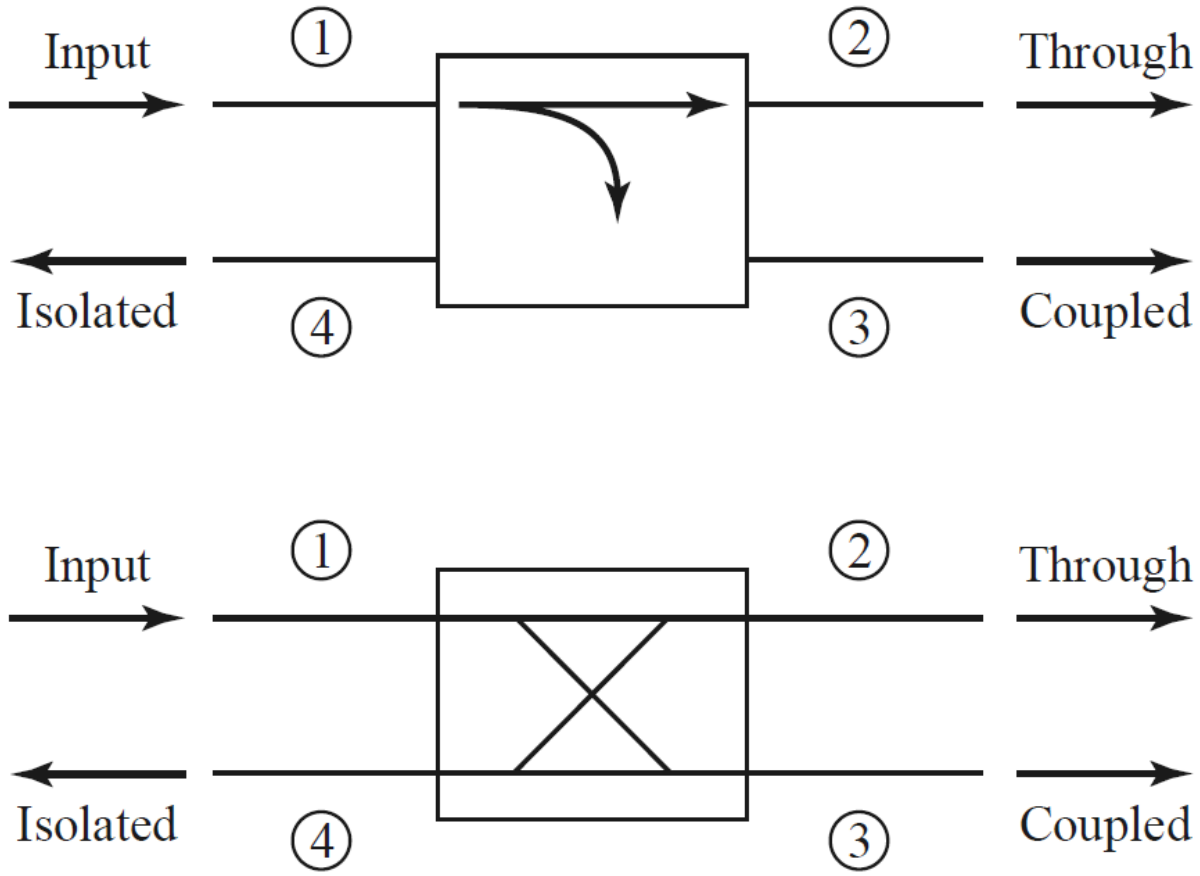

Figure 3.1 Two commonly used symbols for directional couplers, and power flow conventions.

Consider a four-port scattering matrix

$$[S] = \begin{bmatrix} S_{11} & S_{12} & S_{13} & S_{14} \\ S_{21} & S_{22} & S_{23} & S_{24} \\ S_{31} & S_{32} & S_{33} & S_{34} \\ S_{41} & S_{42} & S_{43} & S_{44} \end{bmatrix}$$

For an ideal coupler, this network will be reciprocal, matched at each port, and will have no power delivered to the isolated port. Applying these conditions, the scattering matrix becomes

$$[S] = \begin{bmatrix} 0 & S_{21} & S_{31} & 0 \\ S_{21} & 0 & 0 & S_{42} \\ S_{31} & 0 & 0 & S_{43} \\ 0 & S_{42} & S_{43} & 0 \end{bmatrix}$$

There are two solutions for the ideal directional coupler. First, we have the symmetrical or 90 degree coupler characterized by

$$[S] = \begin{bmatrix} 0 & \alpha & j\beta & 0 \\ \alpha & 0 & 0 & j\beta \\ j\beta & 0 & 0 & \alpha \\ 0 & j\beta & \alpha & 0 \end{bmatrix}$$

Where α and β are the transmission and coupling coefficients, respectively, for the coupler. Inspecting this matrix we see that the voltage wave to the coupled port is 90 degree out of phase with the wave to the through port. For a lossless network, we have

$$\alpha^2 + \beta^2 = 1$$

The second solution is the antisymmetrical or 180 degree coupler characterized by

$$[S]=\begin{bmatrix} 0 & \alpha & \beta & 0 \\ \alpha & 0 & 0 & -\beta \\ \beta & 0 & 0 & \alpha \\ 0 & -\beta & \alpha & 0 \end{bmatrix}$$

There are several terms used to characterize a coupler. First is the coupling C, also termed the coupling coefficient. The coupling relates the coupled power (P_3) to the input power (P_1), that is

$$C = -10\log\left(\frac{P_3}{P_1}\right)$$

If all ports are terminated in matched loads, the coupling coefficient becomes simply

$$C = -20\log\left(S_{31}\right)$$

The insertion loss between the input and through ports is sometimes referred to as main line loss. For matched ports we have

$$IL = -20\log\left(S_{21}\right)$$

The coupler's isolation is a measure of how much input power exits the isolated port. It is given by

$$I = -20\log\left(S_{41}\right)$$

and is ideally infinite.

There are many types of four-port couplers and the one we used is a -3dB coupler, which is also called the quadrature hybrid (or branch-line hybrid) coupler, shown in Fig. 3.2. The quadrature term comes from the 90 degree phase difference between the outputs at ports 2 and 3. Like the ring hybrid, the coupling and insertion losses are both equal to 3 dB.

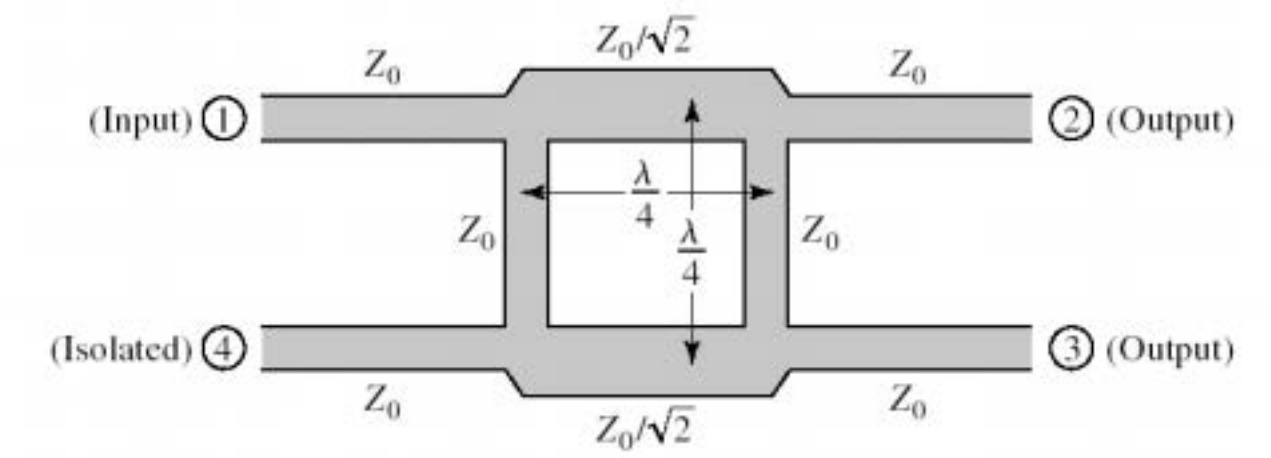

Figure 3.2 Quadrature hybrid (or branch-line) coupler.

The scattering matrix is

$$[S] = \frac{-1}{\sqrt{2}} \begin{bmatrix} 0 & j & 1 & 0 \\ j & 0 & 0 & 1 \\ 1 & 0 & 0 & j \\ 0 & 1 & j & 0 \end{bmatrix}$$

So the quadrature hybrid is a symmetrical coupler.

3.1.2 Design and Simulation

The quadrature hybrid was first designed and drawn in a free PCB software and then implemented into Agilent Advanced Design System (ADS) to do the simulation. The simulation was done at 200 MHz (since the Larmor frequency for 4.7 T is 200MHz) to get S11, S21, S31, S41 parameter and the phase delay between port 2 and port 1, and port 3 and port1. The simulation results are as followed

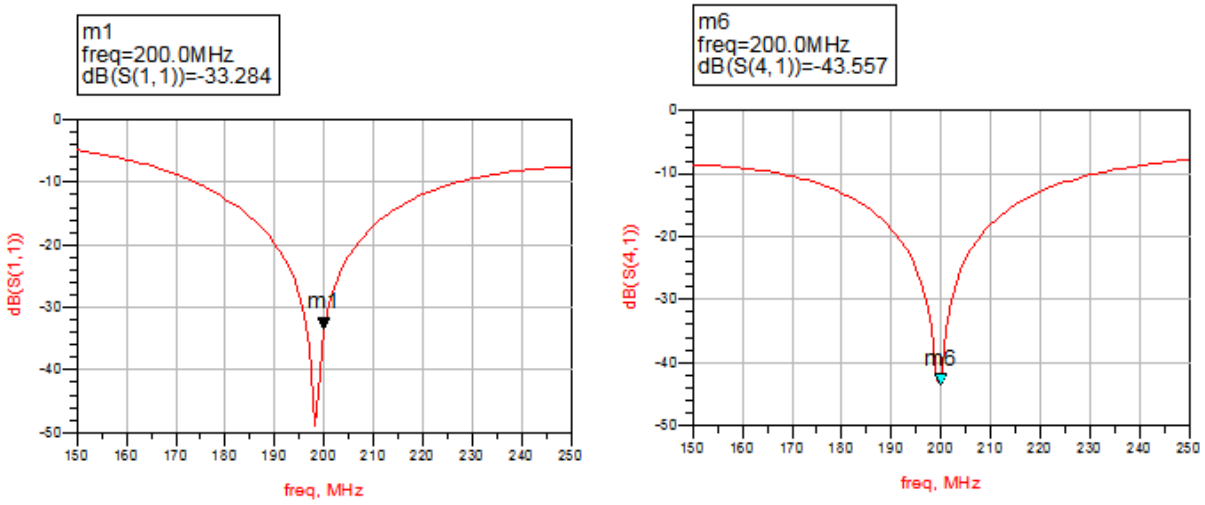

(a) (b)

Figure 3.3 ADS simulation results. (a) S11 parameter of input Port 1. (b) S41 parameter of out put Port 4.

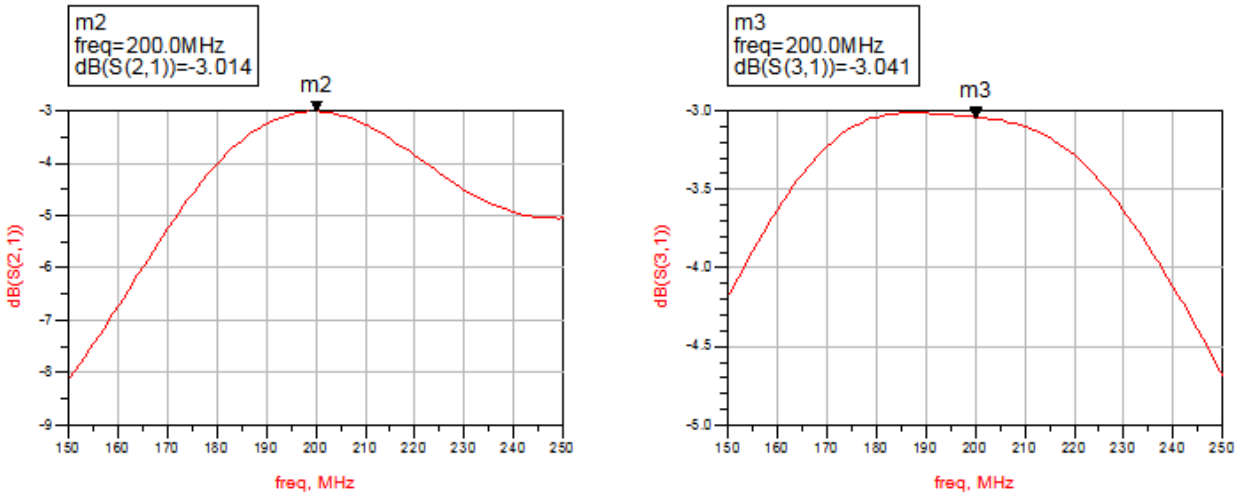

(a) (b)

Figure 3.4 ADS simulation results. (a) S21 parameter of input Port 2 and 1. (b) S31 parameter of out put Port 3 and 1.

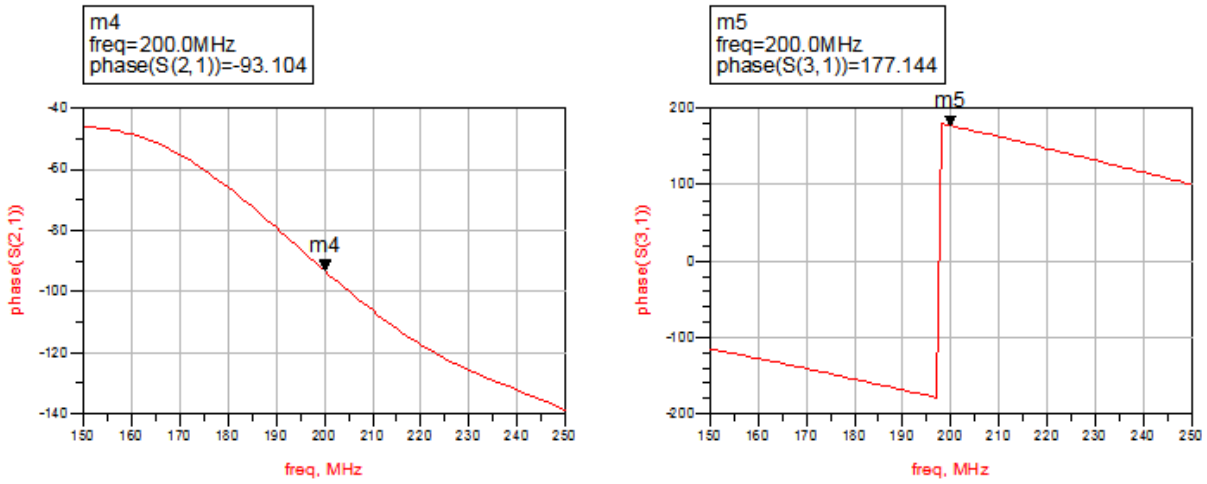

(a) (b)

Figure 3.5 ADS simulation results. (a) Phase of input Port 2 and 1. (b) Phase of out put Port 3 and 1.

Fig 3.6-3.8 show the bench testing results, which correspond very well to the simulation.

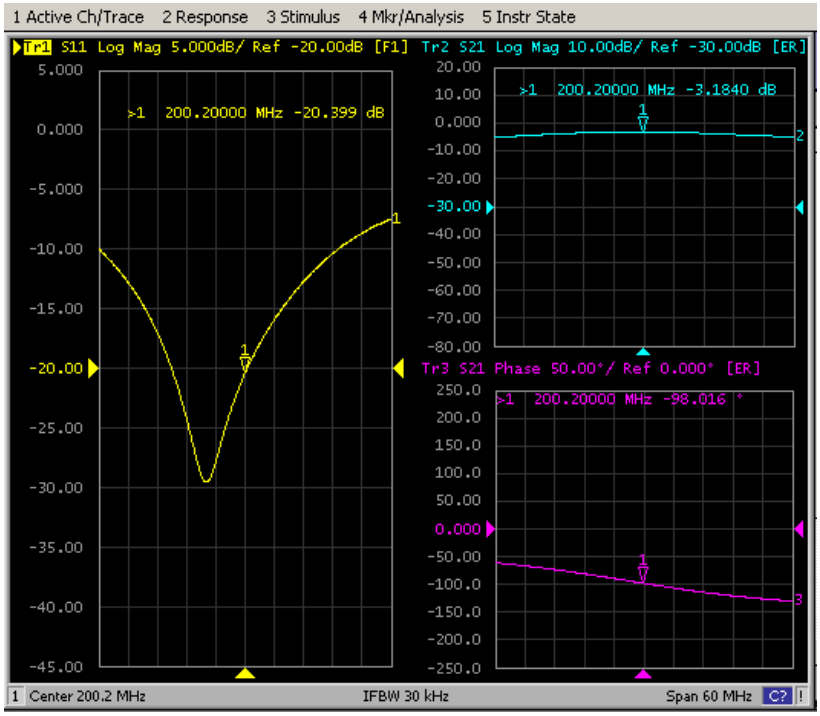

Figure 3.6 S11 magnitude (log), S21magnitude (log) and phase

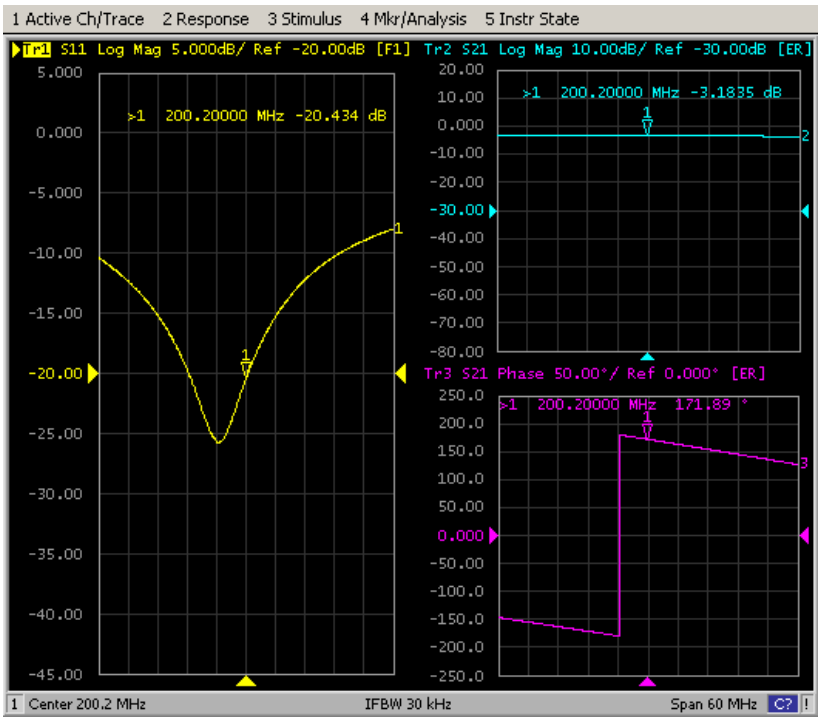

Figure 3.7 S11 magnitude (log), S31magnitude (log) and phase

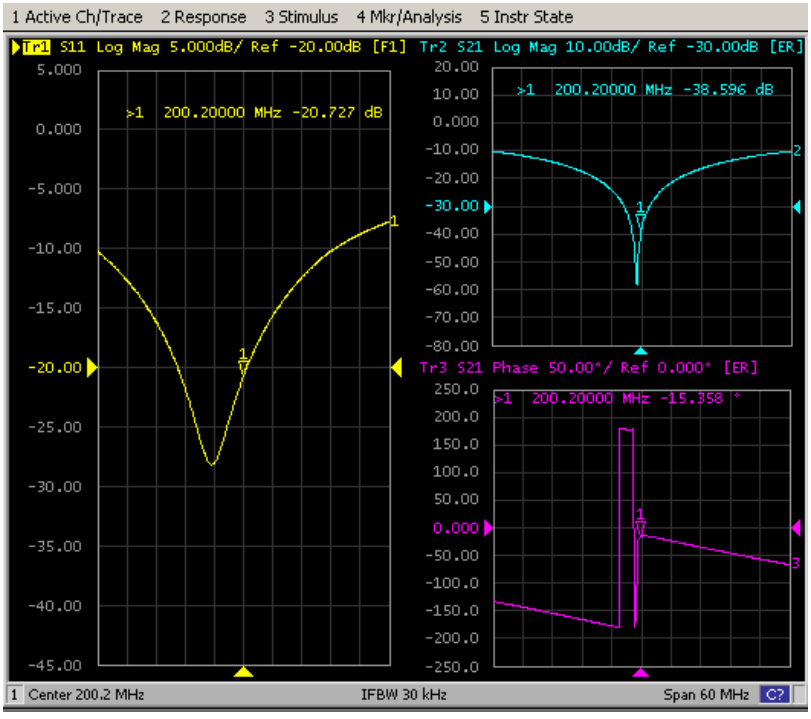

Figure 3.8 S11 magnitude (log), S41magnitude (log) and phase

The hybrid was then made and the value of each component we used with a comparison of that used in the simulation is shown in the form below

Component	Component value (Used in simulation)	Component value (Used in reality)
C_h	22pF	18pF
L_h	28nH	28nH
C_v	15pF	15pF
L_v	39.8nH	39.8nH (part number: 165-03)

Table 1 component value of the hybrid used in the simulation and in reality

3.2 T/R Switch

3.2.1 Introduction

Radio transceiver designers are always faced with a dilemma: how to direct thehigh power transmit signal to the antenna or, in this case, the RF coil, prevent that signal from entering thesensitive front end of the local receiver, while also allowing a low-loss connectionbetween the transmitter and the receiver.

The manner in which this problem is solved depends somewhat on the architecture of the system.Systems that utilize the same frequency for transmit and receive signals, a type of devices configured as transmit/receive (T/R) switches are used to perform thisimportant function.

3.2.2 T/R Switch design

A T-R switch may be simply configured using two series connected PIN diodestogether with some 90 degree phase shifters between the coil and transmitter and an additional set between the coil andreceiver. This configuration is shown in Fig 3.9.

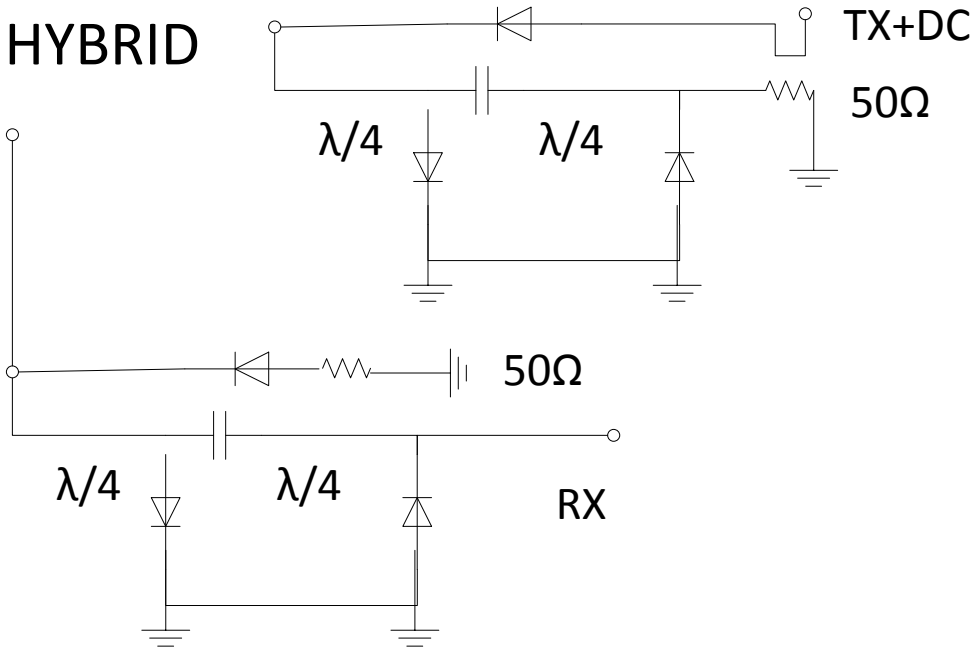

Figure 3.9 Circuit schematic of the combination of hybrid and T/R switch

Bench testing results

The bench testing results are as followed. Since the design combined the T/R Switch and the hybrid coupler, this resultis a combination the both two devices.

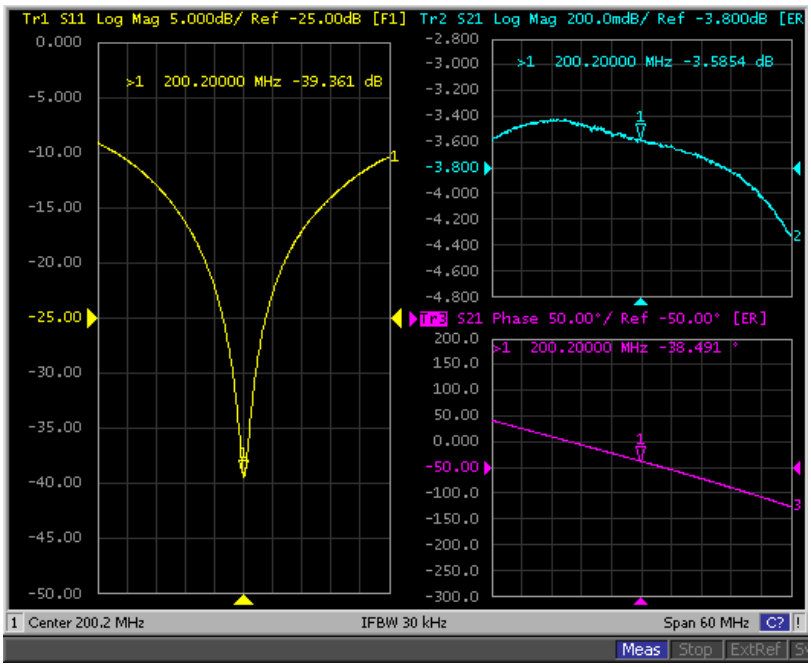

Figure 3.10 Port1: Coil; Port2; RX. S11 magnitude (log), S21magnitude (log) and phase when DC is OFF)

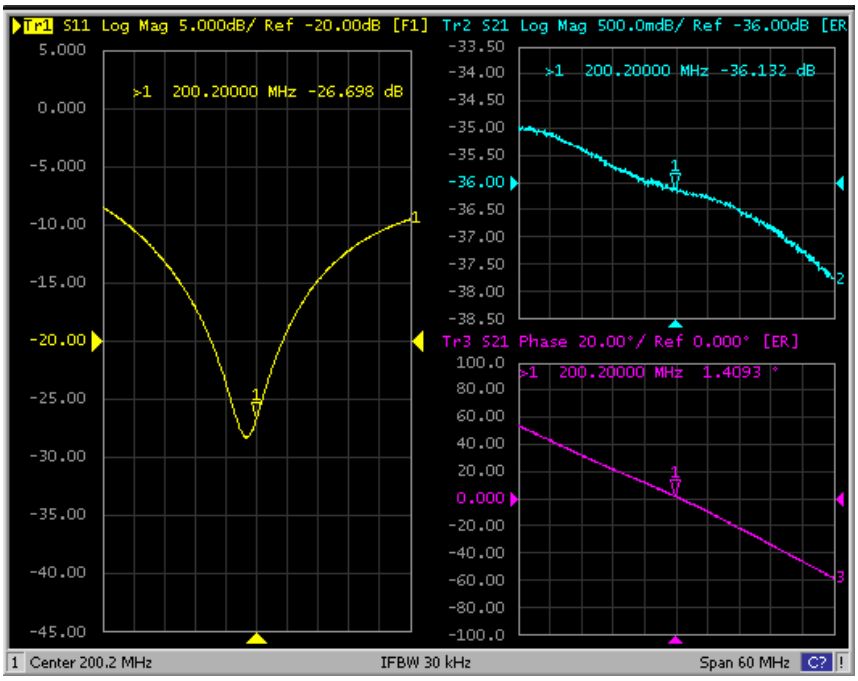

Figure 3.11 Port1: Coil; Port2; RX. S11 magnitude (log), S21magnitude (log) and phase when DC is ON)

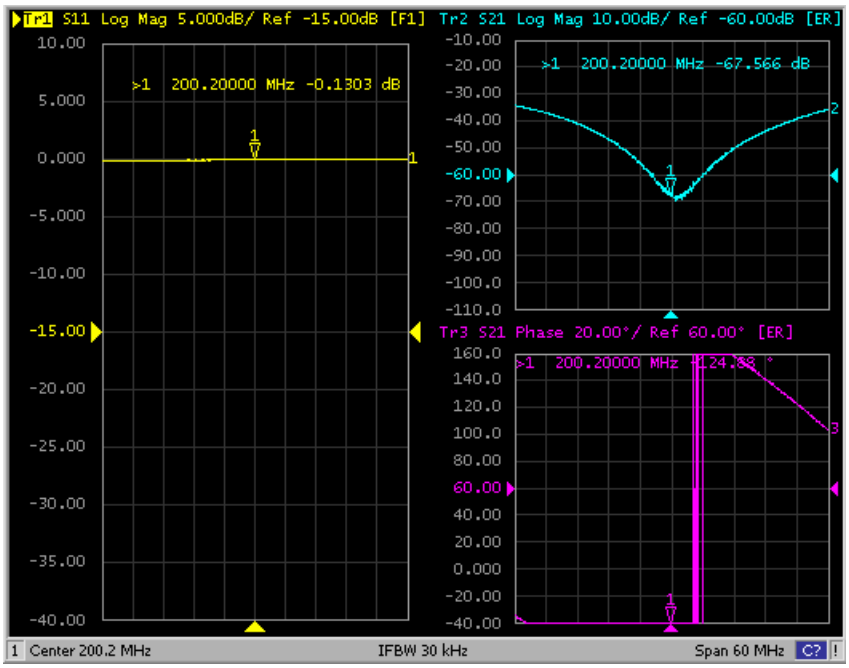

Figure 3.12 Port1: TX; Port2; RX. S11 magnitude (log), S21magnitude (log) and phase when DC is OFF)

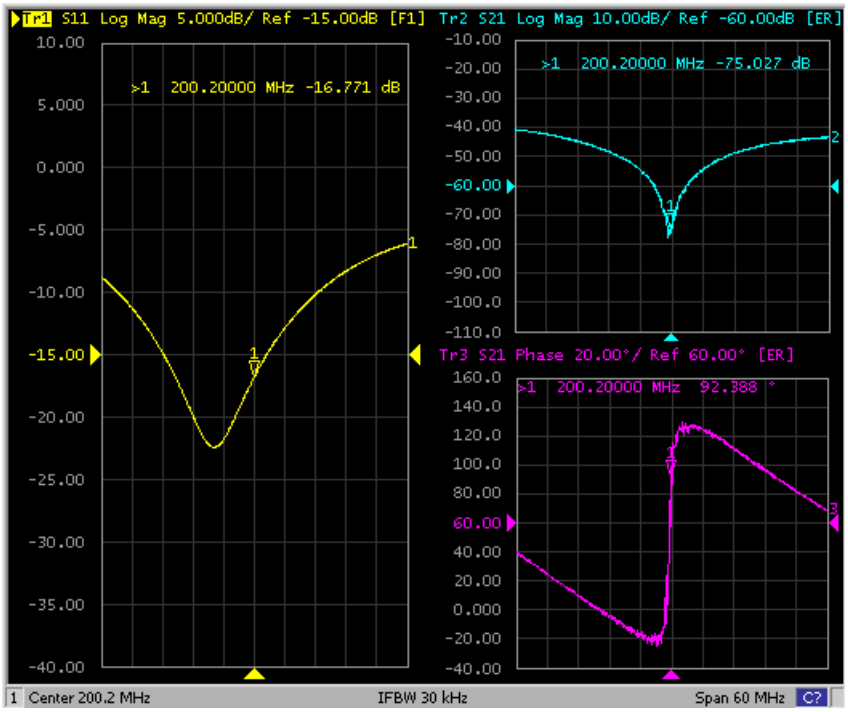

Figure 3.13 Port1: TX; Port2; RX. S11 magnitude (log), S21magnitude (log) and phase when DC is ON)

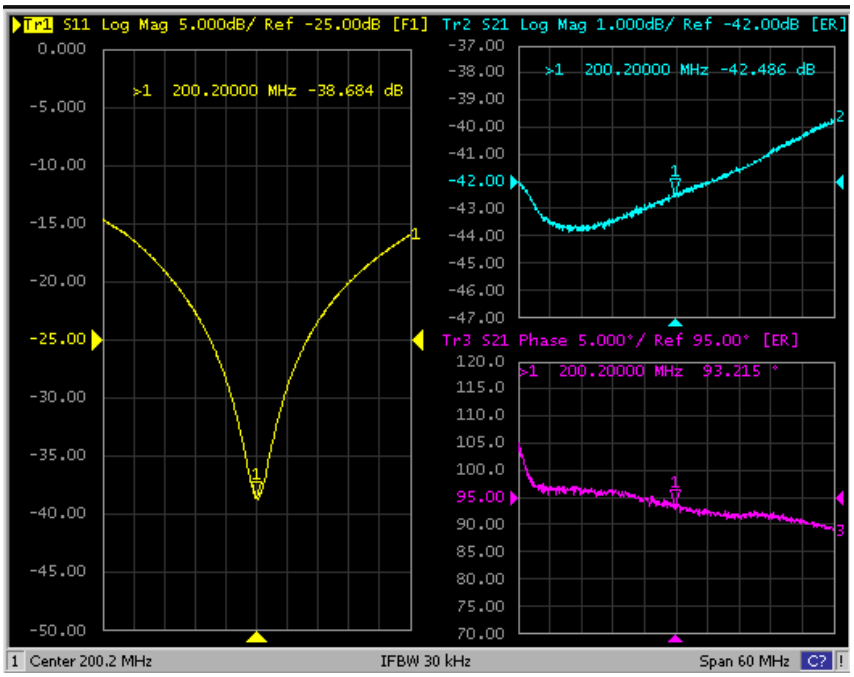

Figure 3.14 Port1: TX; Port2; 50ohm. S11 magnitude (log), S21magnitude (log) and phase when DC is ON)

3.3 Low noise amplifier (LNA)

3.3.1 Introduction

The configuration of a two-stage microwave transistor amplifier is shown in Fig 3.15.The design of a two-stage amplifier usually consists of the optimization of one of the following requirements: (1) overall high gain, (2) overall low noise figure, or (3) overall high power. Certain reflection coefficients are determined to get a desired noise figure and gain performance. Another important issue in the two-stage amplifier is that the stability of the individual stages, as well as the overall stability, must be checked.

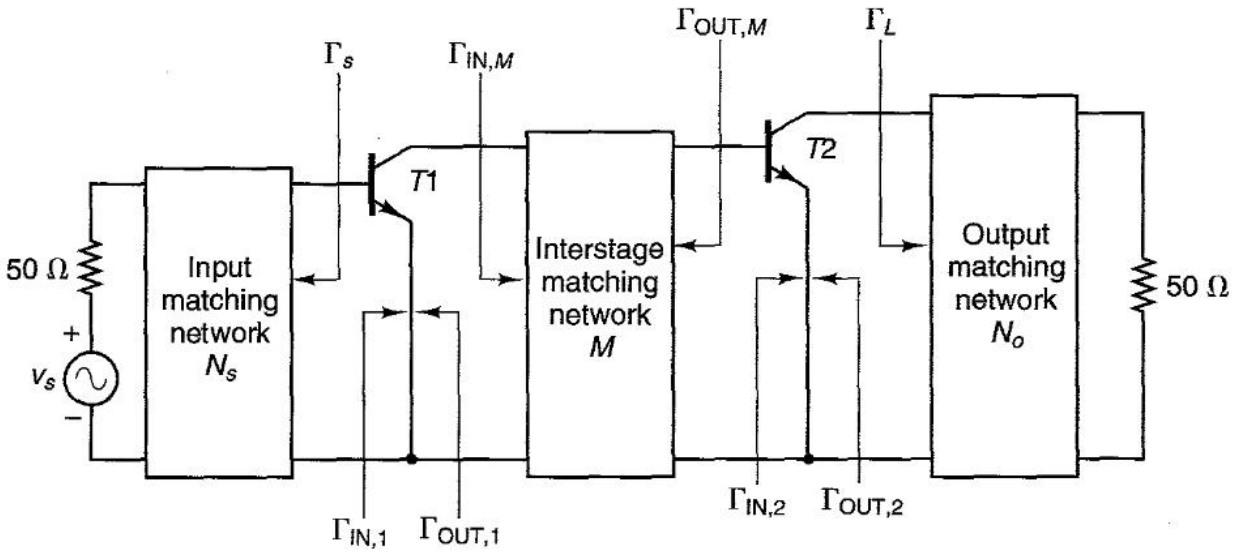

Figure 3.15 Configuration of a 2-stage amplifier design

In some applications the design objective is for minimum noise figure, for example, the 1st stage of our preamplifier design. In theory, the overall noise figure of a two-stage amplifier depends on mainly on the 1st stage. Thus the transistor of the 1st stage is usually selected to have a low noise figure, and a higher noise figure is permitted in the second stage, which was the rule

followed in our amplifier design. A 2nd stage was chosen to enhance the gain performance to the desired value (in the files provided by Siemens, amplifiers with a 25dB gain are recommended) since a minimum noise figure and maximum power gain cannot be obtained simultaneously. Thus trade-offs have to be made between noise figure and gain performance. These will be discussed in this section.

3.3.2 Design and simulation

The circuit schematic was designed based on the two-stage microwave transistor amplifier configuration and drawn in FreePCB software. An ATF54143 FET transistor is chosen for the 1st stage of the amplifier; a BFP720 BJT transistor is chosen for the 2nd stage of the amplifier.

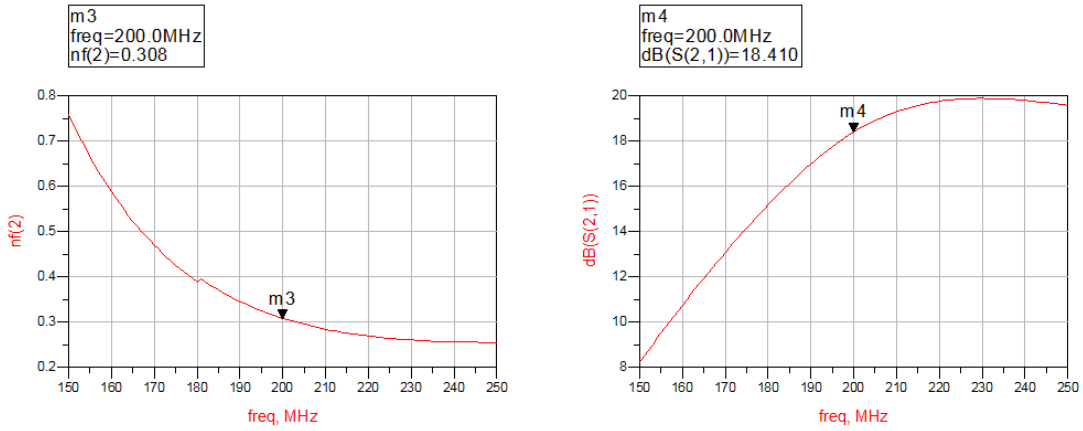

Figure 3.16 Simulation results of the 1st stage LNA. 1) Left: Noise figure. 4) Right: Gain

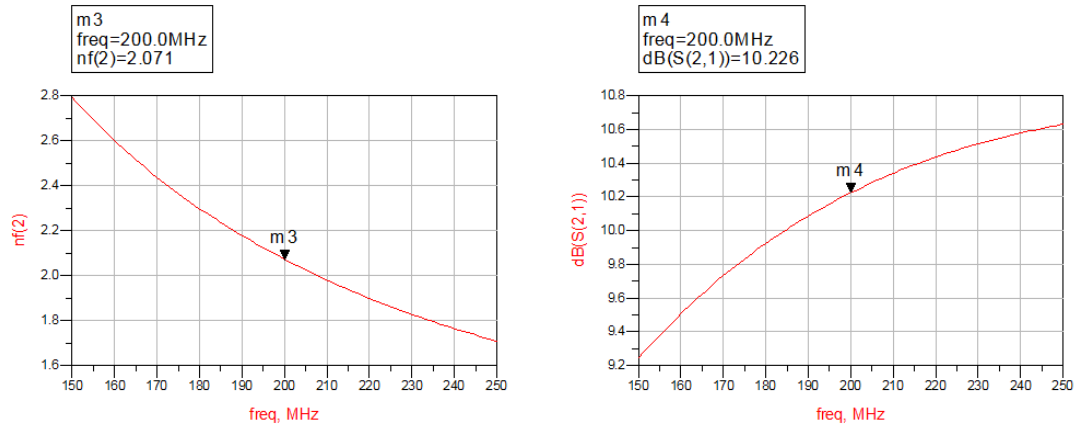

Figure 3.17 Simulation results of the 2nd stage LNA. 1) Left: Noise figure. 2) Right: Gain

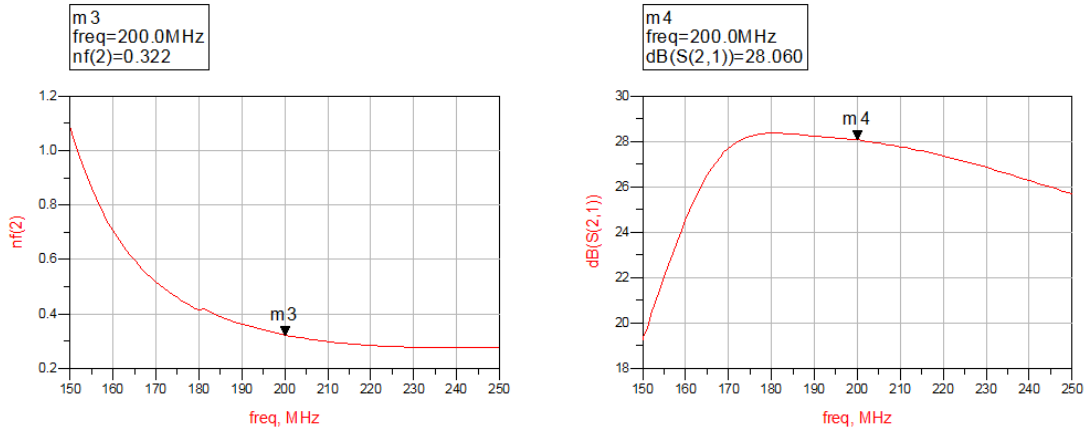

Figure 3.18 Simulation results of the overall 2-stage LNA. 1) Left: Noise figure. 2) Right: Gain

3.3.3 DC biasing Circuit

There are two different types of DC biasing network, i.e., passive and active biasing. The biasing network we considered here in our amplifier design is active biasing. Active biasing is useful to provide a very stable working point with large temperature variations.

The biasing circuit was built with PNP and resistor network. The circuit diagram is shown in the following. It is important to check the I-V curve the PNP to figure out I_c and h_{FE} first. For PNP, V_{BE} is almost fixed at -0.7 V. V_{CE} seems to be a variable. It is better chosen at -5V. V_{GS} is 0.5 – 0.6V for ATF 54143 depending on V_{DS} and I_{DS}.

The Circuit we used is shown in Fig. 3.19.

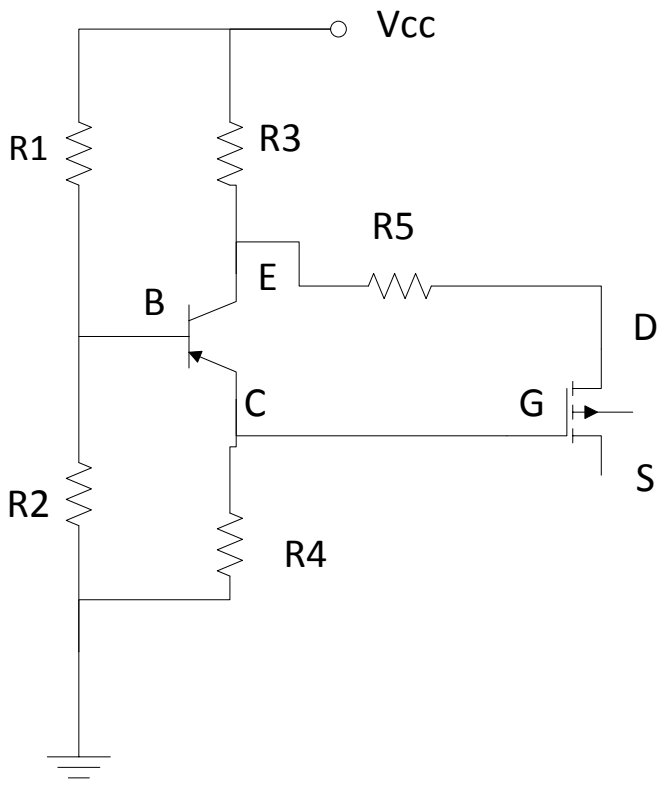

Figure 3.19 DC Biasing Circuit.

3.3.4 Bench testing result

The bench testing result is shown in Fig 3.20, which is very close to simulation result.

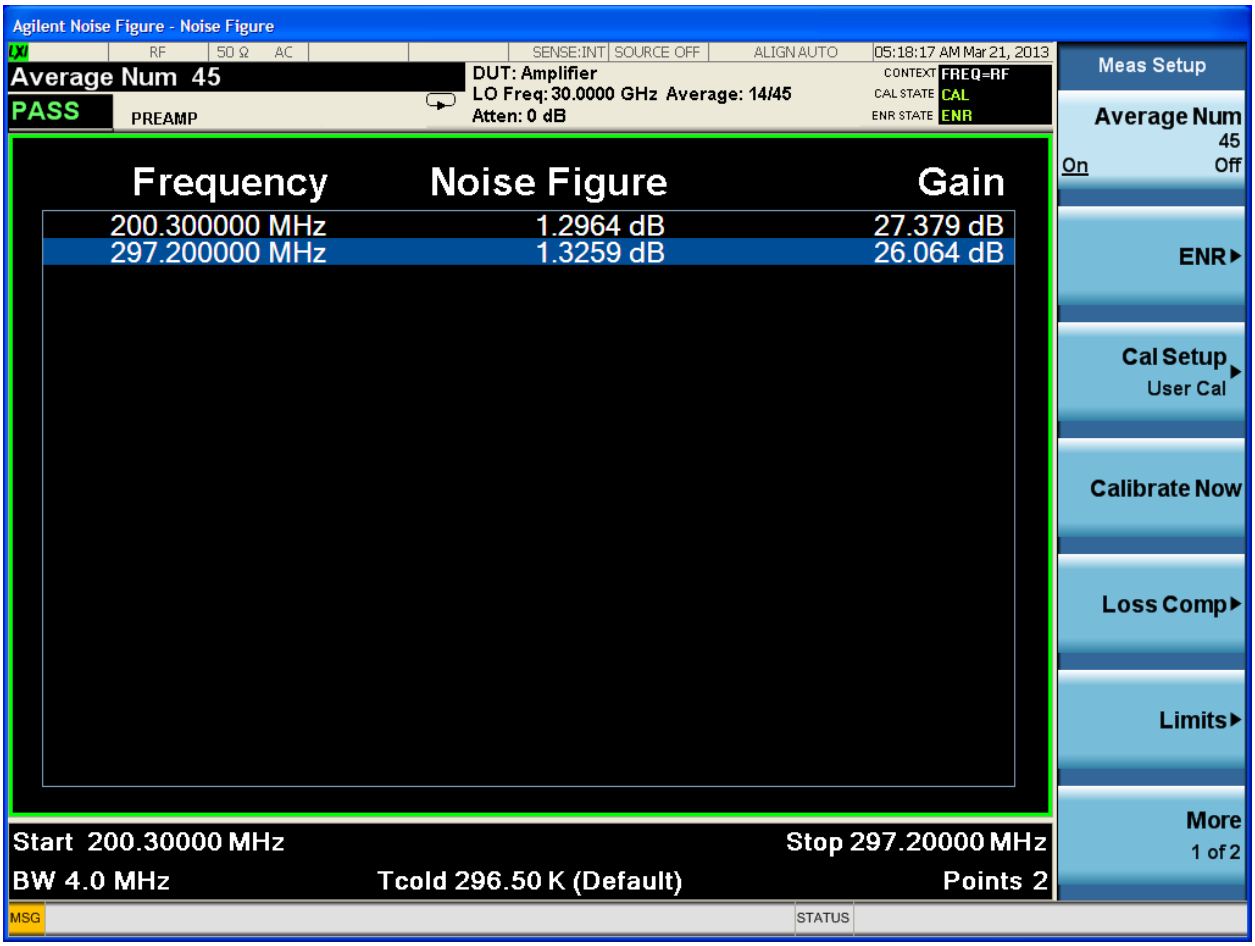

Figure 3.20 Bench testing results. Noise figure and Gain of the amplifier.

Chapter 4

Coil Fabrication and Results

The birdcage coil was fabricated using copper tubes (AWG #16). Copper tapes were used to make the RF shield. However, copper tapes can also be used to build RF coils. In this design, A high pass birdcage was chosen, which means no capacitors were placed on the legs. Moreover, in this case two capacitors in series instead of one were places on the end-ring section between each leg. The reason we did this is because at high field, there will be coupling between the capacitor and the phantom if the capacitor value is too small, e.g. less than 10 pF. So what we were doing was simply double the capacitor value in order to eliminate this undesirable effect.

4.1 Fabrication

The already designed frames of the coil and shieldwere converted into a stl. file using AutoCAD, which is normally a 3d printer readable file type and then printed out by the 3d printer in our lab. A hollow ball of approximately the same size of what we have simulated was printed out as well to be used as the phantom simulating the monkey head for our benching testing. This hollow ball is filled with saline water with a ratio of NaCl and water to be 2.9g/L to mimic the physiology constitution of a monkey head.

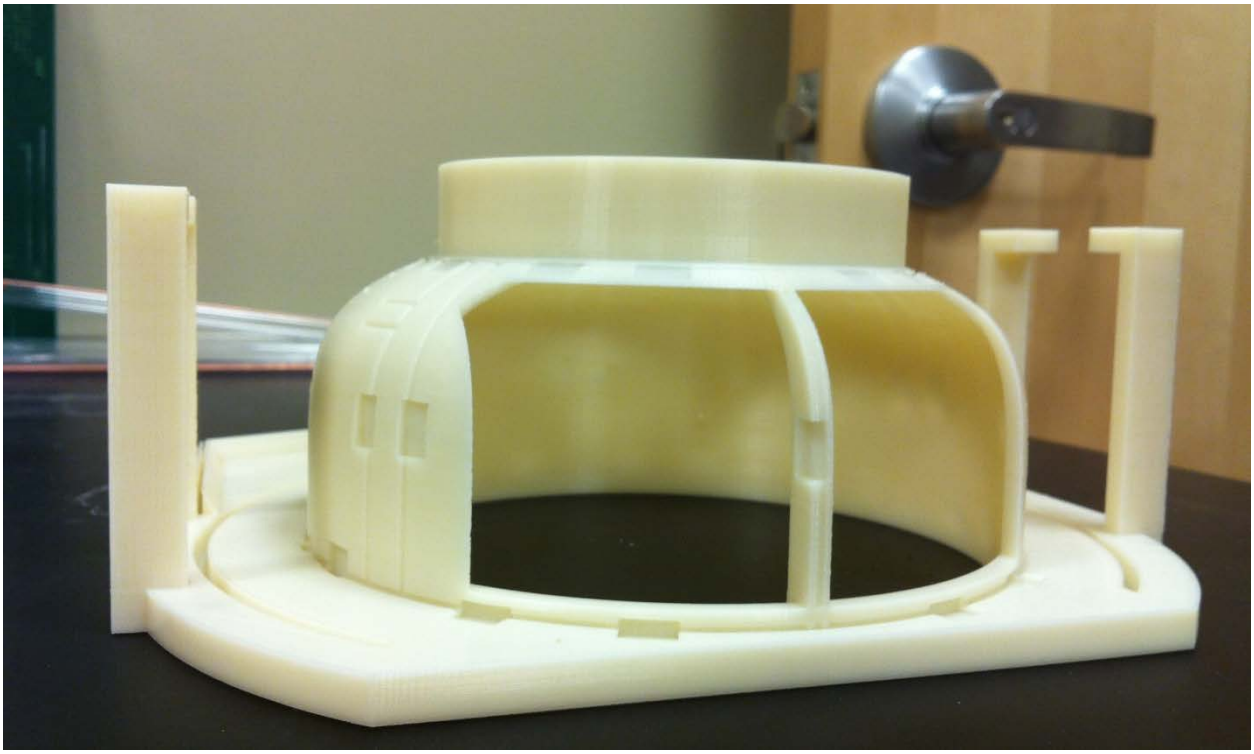

Figure 4.1 Coil frame printed out by 3d printer

The capacitor value we used was 12pF and 4 trimmer capacitors were used (2 for matching and 2 for tuning) to bring the resonant frequency of the desired mode to 200.2MHz (4.7T). The initial value used in the simulation before we split one capacitor into two was 6.8 pF.

4.2 Tuning, matching and decoupling

The dominant mode of the loaded coil was tuned to the resonant frequency by viewing S21 and matched to 50ohms by viewing S11 on the Network Analyzer. For the S21 measurement Port 1 of the analyzer is connected to the input of the coil and Port 2 of the analyzer is connected to a pick-up probe. Like we have discussed, abirdcage coil has (N+2)/2 modes, with N being thenumber of legs. Thus the coil presented has 3 modes, to distinguish the dominant modefrom

the rest a pick-up coil is moved along the central transverse plane. Since abirdcage coil produces highly homogenous field at the center of the coil, when the pick-up coil is moved in the central transverse plane the mode that shows little variation of the received signal is the dominant mode.

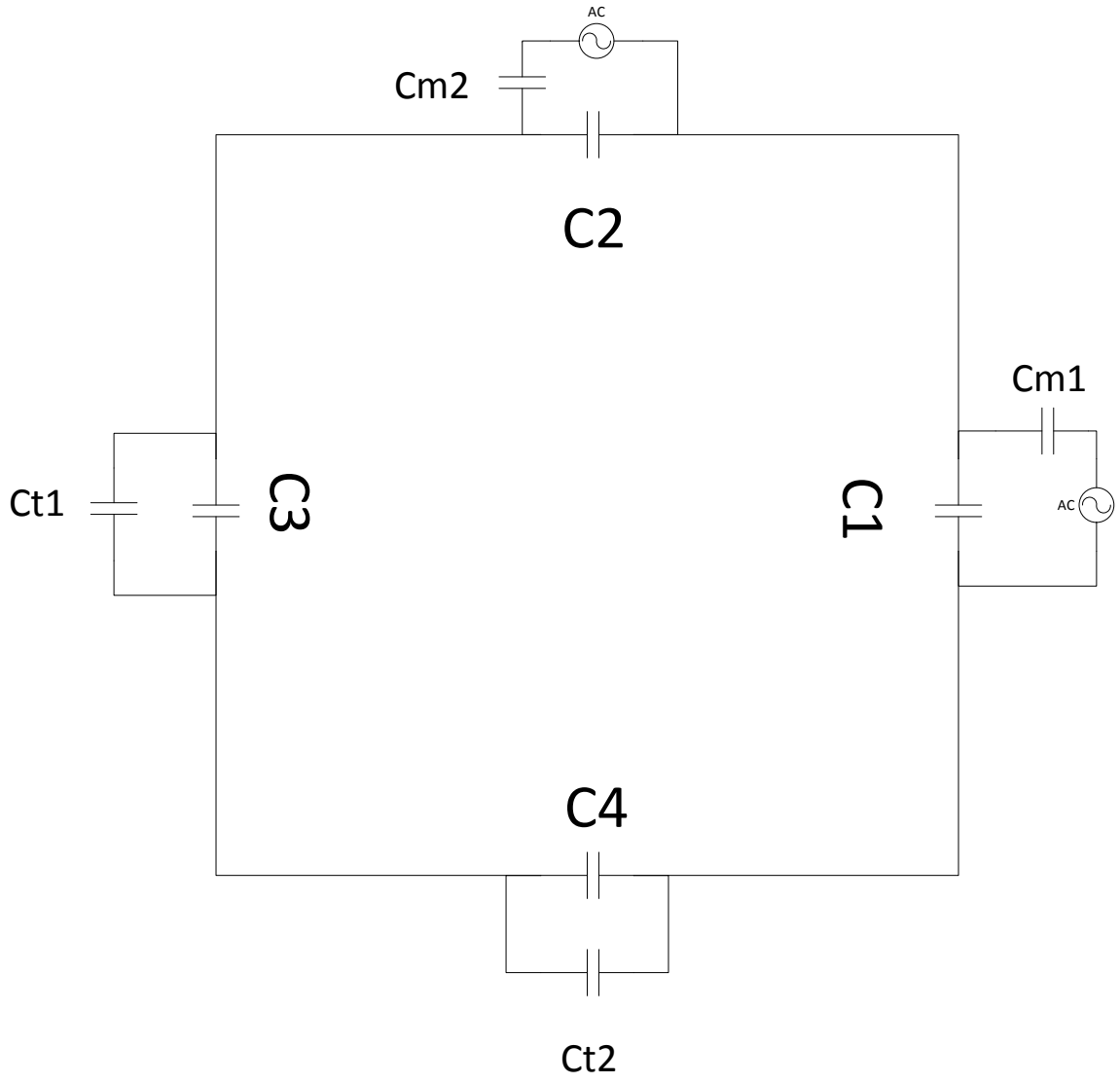

Figure 4.2 The end-ring configuration of the birdcage coil with match and tuning capacitors

Ideally we want all the capacitors to be the same value. In practice, this is not the case because of the variation in the capacitance introduced by tuning, matching and decoupling. The end-ring configuration of the birdcage coil is shown in Fig 4.2, where 4 variable capacitors are added. Two variable capacitors, C_{m1} and C_{m2}, are used to achieve good matching between the feeds and the coil to minimize the reflected power. Another two variable capacitors, C_t and C_{t2} are used to achieve fine tuning because, in practice, capacitors with a desired value are often unavailable thus the constructed coil often has a resonant frequency this is different from the desired operating frequency. Sometimes there is a fifth variable capacitor to achieve good balance between the 2 ports, i.e., to decouple the 2 ports while in this case since it is a 4-ch birdcage coil there is no capacitor placed in between the 2 ports. In reality, the coupling between the 2 ports was minimized due to the structure of this coil. The 2 excited ports were orthogonal to each other, so the interference of the magnetic flux between the 2 loops should be minimal. This results in a natural isolation of the 2 ports.

4.3 Results

The benching testing results are shown in Fig 4.3. The 2 ports of the coil were then connected to the hybrid with the right polarization together with the T/R Switch and Preamplifier. Four cables including the TX, RX, Pin diode DC and Preamplifier biasing DC were connected to the MRI scanner (Fig 4.4).

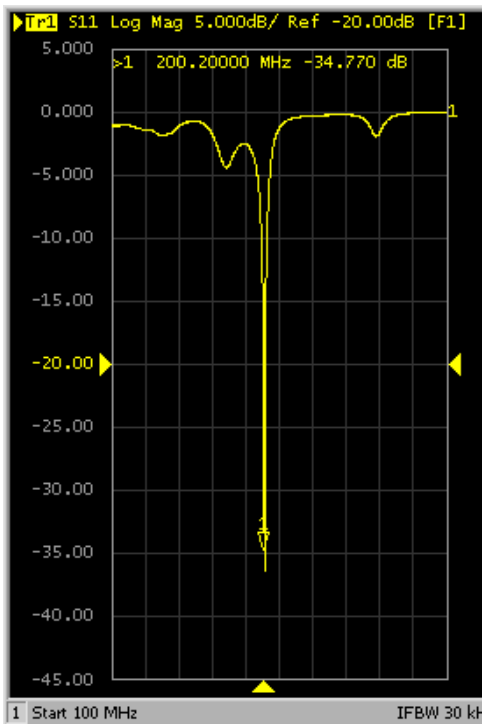

(a)

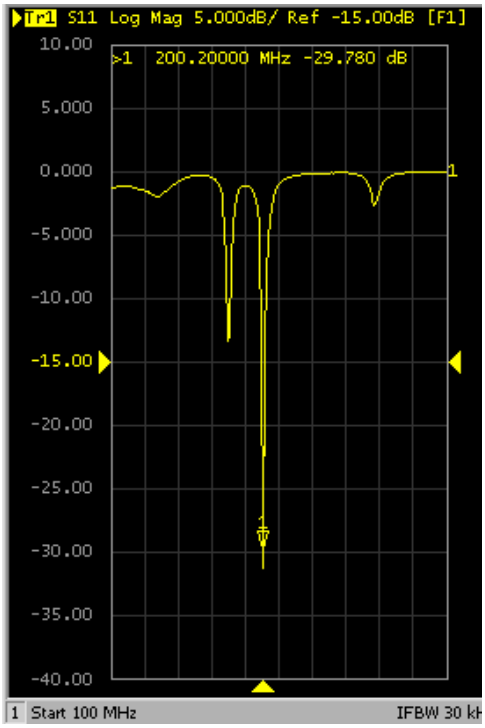

(b)

(c)

Figure 4.3 Benching testing results. (a) S11 of port1 (b) S11 of port2 (c) S21

Figure 4.4 The birdcage coil and a water phantom inside the MRI scanner. (a) Front side view

(b) Back side view

Some MRI scanning images of different orientation were achieved, shown in Fig 4.5.

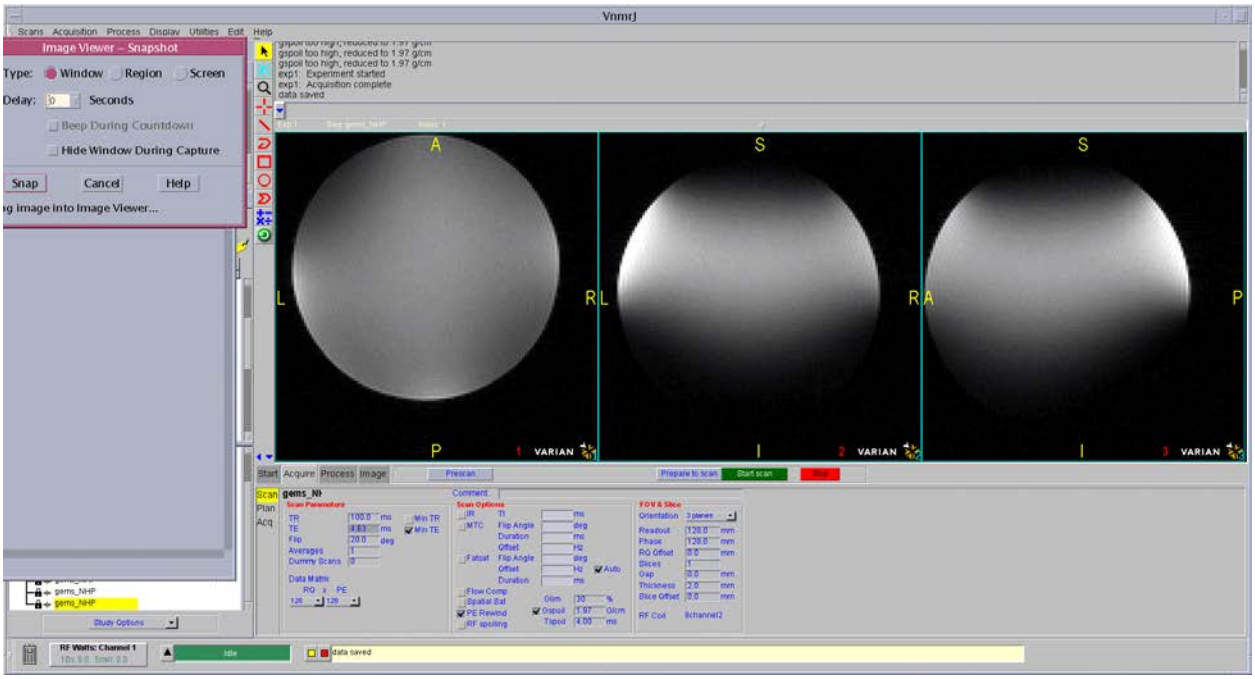

Figure 4.5 MRI images. 1) left: transverse plane. 2) middle: coronal plan. 3) right: sagital plane

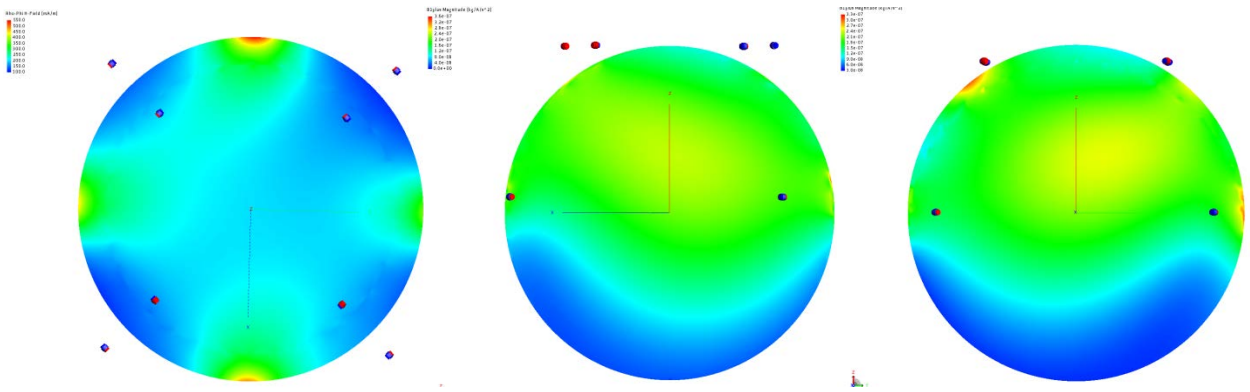

Figure 4.6 A comparison of the previous simulation results.

Chapter 5

Discussion and Future work

In this thesis, a basic concept of a two port drive MRI birdcage coil and briefly how to build it is introduced. Coil size was chosen and simulated in FEKO. And then after the coil was made, it was tuned to 200.2MHz (4.7T), matched and the orthogonal 2 ports ensure the natural isolation between each other. The quadrature nature of the RF output enables an improvement of the signal to noise ratio (SNR).

From the scanning results, we can see that the magnetic field in the central part of the coil was very homogenous andimages of great SNR were achieved. Images from all the three orientations correspond very well to the simulation results.

5.1 Fabrication issues

Some fabrication issues were encountered during this work; they were listed as below and should be considered for the next generation coils.

a) Problems exist such as coil asymmetry. It is very difficult to achieve perfect symmetry in reality and coil asymmetry can cause inhomogeneity issues. Furthermore, it is hard to

achieve the same value for all the capacitors due to tuning, matching and perhaps decoupling requirement.

b) Another problem is that capacitors we used may come with a shift of 5%. They may be replaced with better ones while the price will also be much higher.

c) Last, the model material we used to in our 3d printer is ABS. This type of material is fine for general MRI imaging while for some certain MRI sequences it may cause some inhomogeneity issues. This problem can be solved by replacing the material with carbon Polyamide though the price is higher.

5.2 Future work

An 8-ch transmit and receive phased array coil was attempted after we made this birdcage coil. Decoupling strategies such as overlapping, capacitors using on the shared leg and transformers were introduced on that coil. This time carbon Polyamide was used instead of ABS (Fig 4.6).

Figure 5.1 An 8-ch transmit and receive phased array coil

With this phased array coil, ideally we will achieve a higher SNR compared to the birdcage coil. However, it is far more complicated to make and details will not be covered in this thesis.

References

[1] J. Ackerman, T. Grove, G. Wong, D. Gadian, and G. K. Radda, \Mapping of metabolites in whole animals by 31P NMR using surface coils," NatureVol. 283, 10 January, 1980.

[2] J.M. Jin, “Electromagnetic Analysis and design in Magnetic Resonance Imaging”, Boca Raton, FL, CRC Press, 1988, ISBN – 13 978-0849396939.

[3] Edelstein WA, Schenck JF, Mueller OM, Hayes CE. 1987. Radio frequency field coil for NMR. U.S. patent 4 680 548.

[4] Catherine Westbrook, et al**, “**MRI in Practice”, June 30, 2005, ISBN-13: 978-1405127875 .

[5] “A High-Pass Detunable Quadrature Birdcage Coil at High-Field”, (May 2008). Vishal VirendraKampani, B.S., University of Illinois-Urbana Champaign.

[6] “BIRDCAGE COILS FOR MRI- IN VIVO IMAGING OF 35-CHLORINE AND 1-HYDROGEN NUCLEI”, MALATHY ELUMALAI, The Florida State University.

[7] “Applied Electromagnetics: Early Transmission Lines Approach”, Stuart M. Wentworth, Auburn University, January 9, 2007**,** ISBN-13: 978-0470042571.

[8] “Microwave Engineering”, David M. Pozar, November 22, 2011, ISBN-13: 978-0470631553.

[9] “A METHOD OF MOMENTS APPROACH FOR THE DESIGN OF RF COILS FOR MRI”, Aghogho Obi, WORCESTER POLYTECHNIC INSTITUTE.

[10] “Advanced Parallel Magnetic ResonanceImaging Methods with Applications to MR Spectroscopic Imaging”, RicardoOtazo, University of New Mexico, USA, 2006.

[11] “A 3 Tesla High-Pass Transmit and Receive Quadrature Birdcage Coil For Animal Imaging”, Sep 2012, Xiaotong Sun, Auburn University.

[12] “Multi-channel Coil for MagneticResonance Imaging of Carbon-13 inRats”, April 21st2011, Kgs. Lyngby, Technical University of Denmark.

[13] “Homogeneous and Heterogeneous Resonators in Ultrahigh-Field MRI”, Kyoung-Nam Kim, 07.11.2011, Universität Duisburg-Essen.

[14] “Modeling, Simulation and Optimization of a Microcoil for MRI-Cell Imaging”, BehroozFateh, University of Rostock, Germany, November 2006.

[15] “The Design and Analysis of High Frequency Phased Array Coils for MRI”, Bing Keong Li, University of Queensland in August 2006.

[16] “The Quadrature Hybrid Coupler”, Jim Stiles, the University of Kansas. 4/17/2009.

.

[17] “A High Power Solid State T-R Switch” by Gerald Hiller and Rick Cory, Skyworks Solutions, Inc.

[18] “Low-Noise Amplifier Design and Optimization”, Marcus Edwall, Luleå University of Technology.

[19] “Microwave Transistor Amplifiers: Analysis and Design”, Guillermo Gonzalez, August 30, 1996, ISBN-13: 978-0132543354.